2009-03

Coastal jets and their interactions along the central California coastline

Lynam, Liam J.

Monterey, California: Naval Postgraduate School

NAVAL POSTGRADUATE SCHOOL

MONTEREY, CALIFORNIA

THESIS

COASTAL JETS AND THEIR INTERACTIONS ALONG THE CENTRAL CALIFORNIA COASTLINE

by

Liam James Lynam

March 2009

Thesis Advisor:	Wendell Nuss
Second Reader:	Qing Wang

Approved for public release; distribution is unlimited

THIS PAGE INTENTIONALLY LEFT BLANK

REPORT DOCUMENTATION PAGE		Form Approved OMB No. 0704-0188

1. AGENCY USE ONLY *(Leave blank)*	2. REPORT DATE	3. REPORT TYPE AND DATES COVERED
	March 2009	Master's Thesis

4. TITLE AND SUBTITLE Coastal Jets and Their Interactions Along the Central California Coastline	5. FUNDING NUMBERS
6. AUTHOR(S) Lynam, Liam James	
7. PERFORMING ORGANIZATION NAME(S) AND ADDRESS(ES) Naval Postgraduate School Monterey, CA 93943-5000	8. PERFORMING ORGANIZATION REPORT NUMBER
9. SPONSORING /MONITORING AGENCY NAME(S) AND ADDRESS(ES) N/A	10. SPONSORING/MONITORING AGENCY REPORT NUMBER

11. SUPPLEMENTARY NOTES The views expressed in this thesis are those of the author and do not reflect the official policy or position of the Department of Defense or the U.S. Government.

12a. DISTRIBUTION / AVAILABILITY STATEMENT	12b. DISTRIBUTION CODE
Approved for public release; distribution is unlimited	

13. ABSTRACT

This thesis research focuses on the cause of strong southerly winds around the Monterey Peninsula and particularly on the effects of winter storms that produced strong southerly winds. The high-wind events from 2005 through 2008 were analyzed. During this period, 16 cases were identified that met the criteria of high winds around the Monterey Peninsula. From the 16 cases, three cases were chosen to complete a detailed analysis of the three storm structures.

Results from this research suggest new approaches that improve the prediction of the southerly Coastal Jet on the California Coast that can be accurately predicted. A sea level pressure tool can be used to identify how strong a wind speed gust will be at the Monterey Airport for one storm, and that the Froude number can determine the timing of the onset of winds at the Monterey Airport. When the flow is blocked, (Froude number less than unity) weak winds are observed at the Monterey Airport while stronger winds are seen at the Monterey Airport when the flow is unblocked.

14. SUBJECT TERMS	15. NUMBER OF PAGES
Coastal Jet, Froude number, gap flow, barrier jets, Monterey, windstorm	85
	16. PRICE CODE

17. SECURITY CLASSIFICATION OF REPORT	18. SECURITY CLASSIFICATION OF THIS PAGE	19. SECURITY CLASSIFICATION OF ABSTRACT	20. LIMITATION OF ABSTRACT
Unclassified	Unclassified	Unclassified	UU

NSN 7540-01-280-5500

Standard Form 298 (Rev. 8-98)
Prescribed by ANSI Std. Z39.18

THIS PAGE INTENTIONALLY LEFT BLANK

Approved for public release; distribution is unlimited

COASTAL JETS AND THEIR INTERACTIONS ALONG THE CENTRAL CALIFORNIA COASTLINE

Liam J. Lynam
Captain, United States Air Force
B.S., University of Washington, 2003

Submitted in partial fulfillment of the
requirements for the degree of

MASTER OF SCIENCE IN METEOROLOGY

from the

NAVAL POSTGRADUATE SCHOOL
March 2009

Author: Liam James Lynam

Approved by: Wendell A. Nuss
Thesis Advisor

Qing Wang
Second Reader

Philip A. Durkee
Chairman, Department of Meteorology

THIS PAGE INTENTIONALLY LEFT BLANK

ABSTRACT

This thesis research focuses on the cause of strong southerly winds around the Monterey Peninsula, and particularly on the effects of winter storms that produced strong southerly winds. The high-wind events from 2005 through 2008 were analyzed. During this period, sixteen cases were identified that met the criteria of high winds around the Monterey Peninsula. From the sixteen cases, three cases were chosen to complete a detailed analysis of the three storm structures.

Results from this research suggest new approaches that improve the prediction of the southerly Coastal Jet on the California Coast that can be accurately predicted. A sea-level pressure tool can be used to identify how strong a wind speed gust will be at the Monterey Airport for one storm, and that the Froude number can determine the timing of the onset of winds at the Monterey Airport. When the flow is blocked (Froude number less than unity), weak winds are observed at the Monterey Airport, while stronger winds are seen at the Monterey Airport when the flow is unblocked.

THIS PAGE INTENTIONALLY LEFT BLANK

TABLE OF CONTENTS

I. INTRODUCTION 1
A. SIGNIFICANCE OF BARRIER JETS ALONG THE CENTRAL CALIFORNIA COASTLINE 1
B. OBJECTIVE 3

II. BACKGROUND 5
A. INTRODUCTION 5
B. HIGH WINDS IN COASTAL REGIONS ASSOCIATED WITH BARRIER JETS IN LAND FALLING WEATHER SYSTEMS 5
1. Role of Other Factors 7
C. WIND DISTRIBUTION OVER LAND DUE TO COMPLEX INTERACTIONS WITH TOPOGRAPHY 8
1. Gap Flows and the Resulted Local Wind Speed Maximums 8
2. Flow over Topography and Wind Sheltering in Lee of Topography 8
3. Terrain Induced Pressure Gradient and Local Effects 9
D. FORECASTER'S AIDS TO WIND FORECASTING IN COMPLEX TOPOGRAPHY 9
1. Current Forecast Tools 9

III. DATA AND METHODOLOGY 13
A. DATA 13
1. Surface Observations 13
2. Model Data 14
B. METHODOLOGY 14
1. Creating Categories for Storms 14
2. Synoptic Overview 16
3. Observational Analysis Techniques 16
a. Sea Level Pressure (SLP) Gradient Tool Development 16
b. Mesoscale Effects Discussion on the Monterey Peninsula 17
4. Mesoscale Reanalysis Technique 17

IV. RESULTS AND DISCUSSION 19
A. INTRODUCTION 19
B. SURFACE PRESSURE GRADIENT RELATIONSHIP 19
C. RESULTS FROM EXAMPLE CASES 22
1. Case 1 (January 3-5, 2008) 27
a. Synoptic Overview 27
b. Mesoscale Effects Around the Monterey Peninsula Region 31
2. Case 2 (January 25-28, 2008) 35

a. Introduction 35
b. Synoptic Overview 35
c. Mesoscale Effects Around the Monterey Peninsula Region 43
3. Case 3 (February 23-25, 2008) 49
a. Introduction 49
b. Synoptic Overview 49
c. Mesoscale Effects Around the Monterey Peninsula Region 54
D. SUMMARY OF RESULTS FOR THE THREE CASES 58
V. CONCLUSIONS AND RECOMMENDATIONS 61
A. CONCLUSIONS 61
B. RECOMMENDATIONS 62
LIST OF REFERENCES 65
INITIAL DISTRIBUTION LIST 69

LIST OF FIGURES

Figure 1. Location of the barrier jet along the Central California coastline. 2
Figure 2. Creating a 6 degree radius circle, taken directly from the TR 98-2005 Air Force document. 11
Figure 3. Correlation between wind gust speed, at the Monterey Airport, and pressure difference between Buoy 28 and Buoy 42. The error bars denote a 95% confidence interval as to the expected range of wind gust strength. The predicted wind speed line shows what the expected values for a wind gust given a SLP difference between Buoy 28 and Buoy 42. 21
Figure 4. Wind speed gust at the Salinas Airport, from the pressure difference between the Salinas Airport and the Paso Robles Airport, correlates with wind speed gust (measured in knots) at the Salinas Airport. 26
Figure 5. Storm location at 0000Z on January 4. Contour labels are in pressure in hPa. 28
Figure 6. The storm location at 1200Z on January 4. 29
Figure 7. Infrared Image of the storm as it approaches California on January 4 at 0600Z. 30
Figure 8. Infrared Image of the storm at 1800Z as it approaches California on January 4. 30
Figure 9. Mesoscale low pressure center in the Monterey Bay region at 2200Z on January 4 32
Figure 10. At 1200Z on January 4, the winds were strongest at the Salinas Airport with the winds at 850 hPa showing a strong southerly component. 33
Figure 11. Calculation shows that the winds along with SLP field, at 0000Z on January 5, have a westerly component to them. 34
Figure 12. Display of an upper level trough, in the Gulf of Alaska, which has a 120 knot jet associated with it. A cut-off low is currently right off the central coast of California on January 24 at 0000Z. The red lines are isotachs and the black lines are heightcontours at 500hPa. 36
Figure 13. The upper level trough is now an upper level low with a 120 knot jet moving along the western side of the upper low. 37
Figure 14. A low pressure center value of 995 hPa centered west of California. . 38
Figure 15. The SLP pattern on January 26 at 0000Z. 39
Figure 16. IR satellite image valid at 0000Z on January 26. 39
Figure 17. Multiple low centers in the Pacific Ocean off the coast of California on January 27 at 0000Z. 40
Figure 18. The IR satellite imagery for January 27 at 0000Z. 41
Figure 19. Surface low, making land fall in California, begins to fill rapidly at 0000Z on January 28 42
Figure 20. satellite imagery for January 28 at 0000Z. 42

Figure 21. Winds at 850 hPa coming from a southerly direction with a mesoscale low center west of the Monterey Bay helping the winds to have a slight easterly component at the surface. 44
Figure 22. The wind--increasing over the Monterey Peninsula, at 850 hPa, to around 55 knots by 0600Z on January 26--which helped to trigger the southeasterly winds that occurred at the Monterey Airport at 0800Z with wind gusts approaching 20 knots. 45
Figure 23. Winds at 850hPa from a southeast direction. Notice the alignment of the SLP contours with the coastline of California. The lowest pressure is to the southwest of the Monterey Peninsula. 46
Figure 24. Winds at 850 hPa are from a southeast direction at 0600Z on January 27..... 47
Figure 25. Winds at 850 hPa on January 28 at 0000Z have now switched direction and are coming from the southwest. The switch allows the winds to gain in strength at the Monterey Airport. 48
Figure 26. The deep low to the west of California in the Eastern Pacific Ocean at 1200Z on February 23. 50
Figure 27. IR satellite image for 1200Z on February 23 which displays where the low pressure center is located. 51
Figure 28. The low has moved northeastward over the last 12 hours helping to tighten the pressure gradient over the Central California coastline. The chart is valid at 0000Z on January 24..... 52
Figure 29. IR satellite imagery shows the front moving through the Monterey Bay region of California at 0000Z on February 24, when the strongest winds occurred at the Monterey Airport. 52
Figure 30. SLP field at 1200Z that shows the low continuing to fill and the SLP field maintains its strength over the Monterey Peninsula..... 53
Figure 31. The low pressure center on the IR satellite image at 1200Z on February 24 shows how the low is filling as it continues to the northeast. 53
Figure 32. SLP field at 0000Z on February 25 that shows the low making land fall along the Oregon-California border..... 54
Figure 33. The 850 hPa winds over the Monterey Peninsula (shown with the SLP contours at 1800Z on February 23) have a Froude number less than unity. 55
Figure 34. Winds speeding up over the Monterey Peninsula at 850 hPa on February 24 at 0000Z to 50 knots. Also the low level jet of 50 knots signifies the placement of the frontal boundary at 0000Z on February 24 over the Monterey Peninsula..... 56

LIST OF TABLES

Table 1. The columns are the following: case number on the left, next the surface pressure difference between Buoy 28 and Buoy 42 (ΔP), then highest observed wind speed gust, and last is the difference between the high-wind time at the Monterey Airport, and the time of highest SLP difference between Buoys 28 and 42. A positive time means that the highest SLP difference happened before the highest wind speed while a negative time means that the highest SLP difference happened after the highest wind speed at the Monterey Airport. 22

Table 2. The columns are divided into wind speed, wind direction, wind speed normal to the coastline at 850 hPa, Brunt-Vaisala frequency, and the calculated the Froude number Analysis for the three selected cases. Date and time of all three cases are also given in this table. 24

Table 3. Regression statistics for measured speed and calculated (from pressure gradient) speed. Data are from the Paso Robles and Salinas Airports calculation. 26

THIS PAGE INTENTIONALLY LEFT BLANK

ACKNOWLEDGMENTS

I would like to thank Professor Wendell Nuss for guiding and shaping my thesis research. Without his dedication and knowledge of the complex weather patterns of the Monterey Peninsula, this thesis would have not been completed. In addition, I want thank Professor Qing Wang whose thoughts and suggestions helped with the thesis completion. Also, the data collection by Mr. Bob Creasey helped to move the thesis along in a timely manner. I want to thank Dr. Alvin Larson for his help editing the thesis.

Finally, yet importantly, I want to thank my wife, Celeste, to whom this thesis is dedicated. Her constant encouragement, support, and love enabled me to power through the numerous roadblocks along the way; thank you.

THIS PAGE INTENTIONALLY LEFT BLANK

I. INTRODUCTION

A. SIGNIFICANCE OF BARRIER JETS ALONG THE CENTRAL CALIFORNIA COASTLINE

Strong winds that blow parallel to and along a low-level boundary are called barrier jets (Parish 1982). Barrier jets are found over many different regions in the world, and they are of interest to weather forecasters and boaters (Olson 2007). The weather forecaster's interest in accurately predicting the strength and the timing of the barrier jets along the coastline is important to maintain the public's awareness of how windstorms could affect them in their daily lives. The boater's interest in barrier jets is in planning for increased wind speeds along a coastline and how best to prepare for boating trips in the given area.

The military also has a strong need to know the causes of such strong winds and when strong winds will occur along a given location on the coastline. One good example is with the Coast Guard when called to respond to anglers who are impacted by strong coastal winds. With improved knowledge and forecasts, the Coast Guard could pre-position crews ready to help stranded boaters in rough weather conditions. Another example is coastal operations by the Navy such as inserting some Navy Seals along a given beachhead. If the weather forecaster knows that a barrier jet would occur during the time of insertion, the weather forecaster could more effectively impact the Navy Seals operations, alerting them to the bad weather conditions. Accurate forecast of the barrier jet is also helpful to the forecast of low-level wind shear. If the winds on the lee side of a coastal mountain are light but the winds on the windward side of the coastal mountain are very strong, the possibility of wind shear and moderate turbulence exists in the region around the coastal mountain.

Figure 1. Location of the barrier jet along the Central California coastline.

The barrier jet that forms along the Central California coastline in advance of cyclones has been documented and can be modeled with some accuracy (Doyle 1997). The winds are associated with low-pressure centers and blow from south to north (Doyle 1997). The area where the barrier jets usually blow along the central California coastline is shown on Figure 1 (Doyle 1997 and Google Earth). Not much work has been done on understanding barrier jets along the California coastline, particularly on how they interact and move inland with Pacific Coast storms since the work of Doyle (1997). The work that has been done on barrier jets along the Eastern Pacific Ocean covers the area that extends from the Golden Gate Bridge up to the Gulf of Alaska. Doyle (1997) focused on a single land-falling front and the detailed wind patterns that can occur along the Central California coastline. Ludwig et al. (2006), tried to incorporate a new hybrid modeling scheme to produce better detailed wind forecasts under all weather conditions over the Central Coast of California for a large range of weather conditions. The authors noted, “The hybrid approach

performed best during stable, non-frontal conditions." The new hybrid modeling scheme takes two different models and combines them into one modeling system.

The high winds and detailed flow patterns are an important and challenging forecast problem in frontal situations. The main focus of this study will be to see how the barrier jets associated with fronts and troughs interact with the terrain on the Central California coastline to produce local variations in wind speeds. Neiman (et al. 2004) studied a land-falling front in great detail to see how it impacted the Southern California region. Their findings show "blocking induced frontal splitting and frontal merging, as well as unparalleled documentation of terrain-forced frontal waves," which result in complex flow patterns in coastal orography. Other studies of the region along the Central California coastline deal with precipitation and only some aspects of the wind flow (Ralph et al. 2005; Galewsky and Sobel 2005; Junker et al. 2008).

B. OBJECTIVE

The goal of this study is to assess the mesoscale wind field in the proximity of the coastline of Central California around Monterey Bay that occurs in land-falling low-pressure systems. The primary objectives are to: 1) determine how different structures of storms cause significant wind events along the California coastline; 2) examine factors that cause local variability (e.g., lower wind velocity in Monterey than in the Salinas Valley); 3) develop a forecast-decision tool to aid weather forecasters in making decisions about warnings, etc., when there is potential for strong winds along the California coastline.

Chapter II of this paper provides a background of barrier jets, their interaction with the coastline orography, and the structures of Pacific Ocean storms as they move onto the Eastern Pacific Ocean coastline. Chapter III discusses the data types and data processing methods. Chapter IV presents

case studies of four unique events that happened along the Central Coast of California over the past four years. Chapter V of the thesis has the conclusions and the recommendations.

II. BACKGROUND

A. INTRODUCTION

The airflow around topography is very complex and difficult to understand. Flows affected by topography include downslope windstorms, katabatic flows, mountain breezes, and others. Another type of flow that is mainly modulated by topography is called barrier jets. Doyle (1997) does a great job of explaining the central California coastal topography and its relationship with the airflow.

> The coastal range of central California is one such region where the juxtaposition of the steep coastal orography, moist marine layer, and differential flux forcing can significantly modulate the coastal mesoscale environment. The coastal range of central California comprises five distinct mountain ranges. The Santa Lucia Mountains are located along the coast to the south of the Monterey Peninsula. The Salinas River valley separates the Sierra de Salinas from the Gabilan and Diablo Ranges to the east, with the Carmel River valley located between the Sierra de Salinas and Santa Lucia Ranges. Several regions in these ranges have elevations in excess of 1000 m. The Santa Cruz Mountains are located along the northern portion of the Monterey Bay. The coastline to the south of Monterey is a particularly interesting region to examine the role of orographic modulation of coastal phenomena because of the marked steepness of the coastal range, the proximity of the peaks to the coast, and the near-linear structure of the ridge. The coastal range in this region is mesoscale in character with cross-mountain widths of about 50 km. (Doyle 1997)

B. HIGH WINDS IN COASTAL REGIONS ASSOCIATED WITH BARRIER JETS IN LAND FALLING WEATHER SYSTEMS

Barrier jets have been studied by meteorologists and weather professionals over the past 30 years (Parish 1982; Overland 2007). They are defined in the American Meteorological Society's as "a jet on the windward side of a mountain barrier, blowing parallel to the barrier" (AMS dictionary). Barrier jets have been studied all along the Eastern Pacific Ocean and into the sections of the Western United States of America from California to the state of Alaska

(Galewsky and Sobel 2005; Kingsmill et al. 2006; Olson 2007; Kim and Kang 2007; Neiman et al. 2006; Bond et al. 2005; Neiman et al. 2006; Parish 1982).

In the Pacific Northwest, much research has been done on the modeling of major Pacific Ocean storms to understanding the relationship between storm structure and high winds (Lynott and Cramer 1966; Reed 1980; Mass and Albright 1985; Steenburgh and Mass 1996; Read 2007). These storms include the Columbus Day windstorm (Lynott and Cramer 1966), 1993 Inaugural Day windstorm (Steenburgh and Mass 1996), and the 2006 Hanukah Eve wind storm (Read 2007). It has been documented that, during the Columbus Day windstorm, there were two pressure troughs, and the strongest winds occurred in between these pressure troughs (R. E: Lynott and 0. .P. Cramer 1966). The same structure, i.e., the double dip in pressure tendency, can be seen in all the above studies. Another common feature in these events is seen in the wind direction: winds blowing from the east will switch to a southerly wind when there is a passage of a warm front, an occluded front, or a pressure trough. The winds continue to blow from the south until the gradient relaxes or until the cold front (or trough) on the back side of the low pressure center moves through the region and causes the wind speed to decrease. Wind pattern interactions with the Central California region are not fully understood, given the potential for rather different storm structure further south.

Barrier jets occur anywhere in the world where there are sufficiently high barriers, including the Central California coastline. Barrier jets normally set up along the Central California coastline during the summer months, with the wind parallel to the coastline and from a Northerly direction (Cross 2003). A considerable body of research has examined the summer time barrier jet that occurs under rather persistent synoptic scale conditions. The barrier jets that occur from a southerly direction have not been very well documented in how frequent a barrier jet develops from a southerly direction along the Central California coastline. Southerly jets are typically associated with an approaching

low-pressure system during the winter. These low-pressure systems are transitory and barrier jet conditions can vary considerably over time.

Several factors affect the formation of barrier jets. One apparent condition is the presence of a barrier that is high enough to impede the flow pattern. Another factor is the atmosphere must have a flow of air toward the topographic barrier that is associated with an along-barrier pressure gradient. Overland (2007) suggest that formation of a barrier jet can be identified using the Froude number (Fr). Barrier jets can form when the Froude number is less than unity (Overland 2007). The "Froude number can be calculated from the equation,

$$F_r = U \big/ NH , \quad (1)$$

where U is the low level flow speed perpendicular to the barrier, N is the Brunt-Väisälä frequency, and H is the effective mountain height (Olson 2007)." When the Fr is less than unity, the flow below the barrier top has insufficient energy to flow over the barrier (Olson 2007). Due to this deceleration of the barrier flow, the flow must turn toward low pressure and accelerate along the barrier. This acceleration leads to the formation of a barrier jet. Equation (1) gives an estimate of when the cross barrier flow, for a given barrier height and wind speed, will force flow parallel to the barrier, instead of flowing over the barrier. This effect of impeding the cross barrier flow is referred to as flow blocking.

1. Role of Other Factors

While the Froude number provides a basic measure of the potential for flow blocking and barrier jet formation, the evolution of the cross barrier flow and stability within a given weather system produces some additional factors that influence barrier jet formation and duration. Barrier jets have been shown to develop with frontal systems (Doyle 1997 and Neiman et al. 2004). It is not known, however, whether other weather system structures could also allow for the development of a barrier jet. The direction of the flow towards the topography determines the cross barrier component, which may help or inhibit

the formation of a barrier jet along the Central California coastline. Since only a single case analysis has been done on a barrier jet that developed along the Central California coastline (Doyle 1997), the sensitivity of their intensity, duration, and occurrence is not known.

C. WIND DISTRIBUTION OVER LAND DUE TO COMPLEX INTERACTIONS WITH TOPOGRAPHY

1. Gap Flows and the Resulted Local Wind Speed Maximums

Gap flows are known to occur in many different places in the world and in the state of California (Zhong et al. 2008 and Neiman et al. 2006). Flows through topographic barrier gaps are also known to produce strong winds that blow mainly parallel with the gap. These gap flows may also arise in land falling systems to produce local wind maxima. Wind speed maximums have been observed in the gap exit region of gap flows (Colle and Mass 2000, Colle and Mass 1998, and Lackmann and Overland 1989). The role of gap flow in the Salinas River Valley forms a gap that may contribute to high winds near the coast. This has not been adequately studied to determine how the wind structure in the valley develops and evolves through the river valley and impacts the local wind patterns in land falling systems.

2. Flow over Topography and Wind Sheltering in Lee of Topography

Air flow around topography is a very complex issue. When all the low level air flows over topography, the Froude number is greater than unity. When the Froude number is less than unity, the low level air flow will be blocked (Doyle 1997). The topography plays a very important role in the development of barrier jets. The complex topography of the Monterey Bay region can consequently produce a rather localized wind response that depends on the Froude number. As noted by Doyle (1997) and others, flow blocking by topography can result in both up and downward stagnation. On the upwind side, this stagnation can turn into a barrier jet as the flow accelerates along the barrier. Downstream of the

barrier an area of weaker winds tends to be produced by the flow stagnation. The detailed character of the response will depend upon the flow evolution near the complex topography of the Monterey Bay region.

3. Terrain Induced Pressure Gradient and Local Effects

Terrain induced pressure gradients also occur as the flow interacts with the topography. For flow over topography the upstream ascent and downstream descent tend to produce windward ridging and lee troughing. Doyle (1997) suggests at the possibility that the blocked flow can have windward ridging and a lee trough, which result in localized wind maxima. The result of these localized pressure perturbations is to produce mesoscale pressure gradients that may result in local wind accelerations and decelerations. The degree of wind enhancement due to land pressure variations in a barrier jet along the Central California coastline has not been systematically examined. Doyle (1997) investigated one such storm and found out that the mesoscale response to steep coastal topography results in a 45% enhancement to the near-surface jet strength. Other barrier jets that occur along the Central California coastline have not been examined to determine the degree or nature of this enhancement.

D. FORECASTER'S AIDS TO WIND FORECASTING IN COMPLEX TOPOGRAPHY

Wind speed has always been a difficult weather forecast parameter to predict. Wind speed predictions in computer models have improved over the last 30 years with the numerous upgrades that have taken place in modeling centers. The accuracy of predicting wind speed is much better than it used to be, but it still is not perfect and sample tools provide useful checks against model guidance.

1. Current Forecast Tools

A tool for predicting wind speed from pressure gradients, calculated from pressure difference between measurements stations, has been proposed (AF TR

98-002 year 2005). Many weather “rules-of-thumb” have been created to predict the strength of the wind speeds in a given area. For example, in the Pacific Northwest, the Central Weather Service Unit has a webpage that correlates sea-level pressure differences between locations to wind speeds at Sea-Tac International Airport (ZSE website).

The Air Force also uses pressure gradient tools to predict wind speeds, and the method states that one needs at least two pressure measurement stations (TR 98-2005). The Air Force gradient method details a six-step approach in predicting wind speeds. The first step is as follows, “Create a 6°-latitude radius circle with the forecast location at the center” (Figure 2). The second step is to obtain the air pressure at the location for which a wind forecast being made. The third step is to find the pressure at the edge of the circle in a direction at right angles to isobars. In the fourth step, the difference in pressure (millibars or hPa) between the forecast location, at the center of the circle, and the point at the edge of the circle is calculated. The fifth step uses “the numerical difference, in millibars, to calculate the wind speed in knots” such as, for example, a 20 hPa difference would predict to 20 knots for the maximum wind speed that can occur with this pressure gradient. Next, take 50% of the gradient wind speed to estimate a sustained wind speed that is likely to be observed. To calculate daytime peak gusts for the wind speed take 80 to 100% of the gradient wind to estimate the speed of a wind gust. The Air Force manual does not state the accuracy of this method and is somewhat simplistic in its approach. Also, the technique does not account for topography interactions with the wind flow. This approach assumes that the maximum wind speed which occurs when it is in gradient balance with the pressure gradient. For situations like the barrier jets, the flow tends to be highly ageostrophic and wind speeds can potentially exceed this gradient balance estimate. Under down gradient flow such as the barrier jet or gap winds, the pressure difference or gradient may correlate with wind speed. This will be examined in this study.

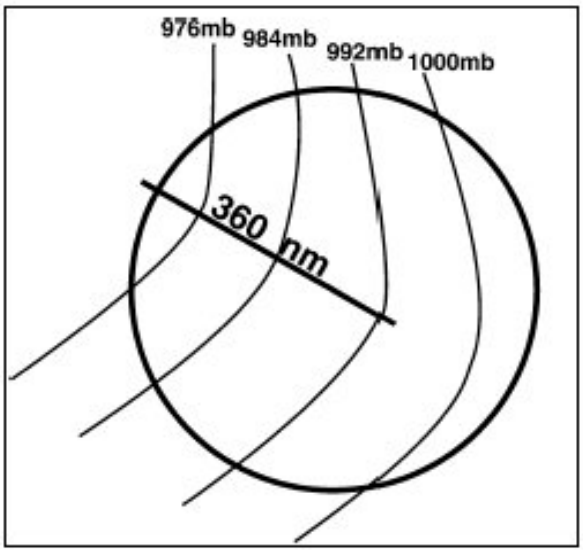

Figure 2. Creating a 6 degree radius circle, taken directly from the TR 98-2005 Air Force document.

THIS PAGE INTENTIONALLY LEFT BLANK

III. DATA AND METHODOLOGY

A. DATA

The data used for this study were obtained from many different sources primarily obtained through World Wide Web. The data sources can be divided into two separate categories: surface observations and model data. Both data types were used extensively for this study to gain further understand the characteristics of air flow interacting with topography.

1. Surface Observations

The surface observations came from three different sources. The first was the observational database archived by the Air Force 14th Weather Squadron for previous years. This Air Force 14th Weather Squadron's database was used to examine conditions at the Monterey (KMRY), Salinas (KSNS), and Paso Robles (KPRB)' airports. The data was gathered in the METAR format from the 14th Weather Squadron's website. The second source used for surface observations came from the National Data Buoy Center (NDBC) database. The surface observations chosen from the NDBC were made on buoys 59, 28, and 42 (NDBC). The data format is the so-called "Standard meteorological data" and was used for all three buoys (NDBC). The third source was the Meteorological Assimilation Data Ingest System (MADIS) historical observations (http://madis.noaa.gov/). The observations were used here in a mesoscale reanalysis technique to depict local wind structures.

With these data sets, quality control was done to ensure that the data did not have any significant errors. A couple of errors were noted with the Monterey and Salinas Airports' weather observations. One error was the Monterey observation (for one case) had wind speeds that were recorded as being 125 knots for six hours. Because of this error, a decision was made not to use this case for an in depth case study analysis. In addition, there is missing data at the

Salinas Airport during a couple of the weather events. This loss of data may have been the result of a possible power outage, at the airport, caused by the ferocious winds.

2. Model Data

The model data, which was used for this study, came mainly from the North American Mesoscale (NAM) model output from the years of 2005 thru 2008. Also, the Global Forecast System (GFS) weather model output, for years 2005 thru 2008 was used in this study. Of the 17 case studies from the 2005-2008 timeframe, three cases were chosen for the months of January and February in the year of 2008 for more detailed analysis. The NAM model, at that time, was referred to as the Weather and Research Forecast Model (WRF version 2.2.1), which was being used by the National Center for Environmental Prediction (NCEP) modeling center. In April of 2008, NCEP started using version 3.0 for the WRF weather model, which was not used for this study (NCEP). The model grid spacing used for this model was 32 kilometers. The GFS model outputs, as well as the Fifth-Generation NCAR/Penn State Mesoscale Model (MM5) model outputs, were compared with the NAM model results. The NAM model had the best initialization for all systems, which were examined in great detail. The NAM model also had some issues because it did not show strong enough winds through the Salinas valley and at the Monterey Airport. To address these issues, a mesoscale reanalysis technique was done, which will be described in a later section.

B. METHODOLOGY

1. Creating Categories for Storms

To identify a barrier jet wind event, a proposed set of meteorological conditions needed to be met. The first condition was the presence of high winds along the coast as well as inland locations. The last four years of weather observations at the Salinas Airport were used with standards requiring that the wind speed at Salinas Airport [and elsewhere] needed to have a gust of at least

30 knots. After identifying 18 potential cases, where the wind gusted from a southerly direction, buoy observations were used to select those where the wind direction came from the south and the wind speeds were greater than 30 knots. All cases identified met those criteria.

Upon further investigation, the cases could be classified into two general categories. The first category, and the one most prevalent, is the land falling frontal systems. This category shows a basic pattern where wind speeds begin, in each case, very weakly but, as the frontal system approaches the winds ahead of the cold front begin to ramp up and wind speeds can become in excess of 40 knots at Monterey and Salinas Airports respectively. The second category, the one that did not happen as frequently as the first, is the cut-off low or dropping low case. In this category, the weather system does not have clearly defined frontal features but instead has short wave troughs embedded within the system that rotate around the low-pressure center. With these two classifications, the next step is to see the frequency of occurrence of each type. There were 18 events that happened from January 2005 through March 2008. Of the 18 events, 12 were classified as land falling frontal system types. There were only five cut-off low cases. One case was deemed to be not a great example for a land falling frontal system, because, for that case, the only time the wind speeds jumped above 30kts was at frontal passage (or well behind the front) and the winds were mainly from the west to northwest direction.

Three storms were then further investigated to see the similarities and differences between them. The storms were chosen for their unique characteristics that produced high winds around the Monterey Peninsula. Case 1 was chosen because the winds were very strong over the Monterey for over 12 hours in duration, and it was associated with a frontal system moving through the region. Case 2 was chosen mainly because it affected the Monterey Peninsula for four days and represented a dropping low example. Also case 2 fit the definition of a cut-off low that stalled in the Eastern Pacific Ocean, off the coast of California. Case 3 was chosen because it was another frontal system case;

however, this frontal system moved very quickly through the Monterey Peninsula (less than six hours for the high wind part). The three cases represented the main systems that had a tendency to produced strong southerly winds around the Monterey Peninsula.

2. Synoptic Overview

Synoptic overviews were done to characterize the basic evolution of three representative storms: January 3, 2008 – January 5, 2008 (case 1), January 25, 2008 – January 28, 2008 (case 2), and February 23, 2008 – February 25, 2008 (case 3). The synoptic overview describes how the storms formed and affected the weather in the Eastern Pacific region. The locations of the surface low pressure regions, associated with the individual storms, and their temporal evolutions were examined to determine what types of coastal and topographic interactions.

3. Observational Analysis Techniques

a. Sea Level Pressure (SLP) Gradient Tool Development

Since the surface wind is fundamentally related to the SLP gradient, the SLP differences between stations were examined to determine its potential utility for determining the local wind speeds. This SLP tool takes two different weather stations and calculates the pressure difference between them in millibars (hectopascals or hPa) at a given point in time. Once a number is derived from the two stations it is then compared to the wind gust at a weather station to see if there was any correlation between the two quantities. This technique was used on 16 of the 18 weather cases identified in the study and used the following five locations: Buoy 42 which is located at 36.789N, 122.04W, which is 27 nautical miles west of Monterey Bay, California (NDBC); Bouy 28 which is located at 35.741N, 121.884W, which is 55 nautical miles to west by northwest of Morro Bay, California; the Monterey Regional Airport which is

located at 36.587N, 121.843W, the Salinas Regional Airport 36.663N, 121.606W; and the last station used was Paso Robles Regional Airport which is located at 35.673N, 120.627W.

b. Mesoscale Effects Discussion on the Monterey Peninsula

To determine mesoscale or local variations in wind, observations were examined over the evolution of the three cases that were chosen for further investigation. The time evolution of flow blocking was compared to the wind response at the three locations (Buoy 42, the Monterey Airport, and the Salinas Airport) to highlight any distinct relationships that might be observed at those locations.

Flow blocking is calculated using the Froude number (equation 1) with the wind speed taken from model output at the 850hPa level. Here, the Brunt-Vaisala frequency was obtained from the model output, the height of the barrier (in this case the Santa Lucia Mountains) was taken to be 1,000 meters. If the Froude number is less than unity the flow is considered to be blocked, while the Froude number greater than unity is considered to be in an unblocked response. Then the magnitudes of the wind in the onshore and along shore direction were calculated. Based on the direction of the coastline, the onshore and along shore components of the wind were defined as those at 240^{o} and 150^{o} wind direction, respectively.

4. Mesoscale Reanalysis Technique

To fully characterize the mesoscale response of the wind field, a mesoscale reanalysis was done using all available surface observations and the NAM model as a first guess field. This mesoscale reanalysis was done using multiquadratic (MQ) interpolation (Nuss and Titley 1994) to blend model first guess values with available surface and upper air observations. The MQ technique was applied in three dimensions, to account for the elevation of surface observations in topography could be accounted for. Observations and

model error characteristics were used to weight the observations and model points relative to each other in the analysis. In general, the observations were given greater weight in the analysis but if no observations occur in a region then the model value is given full weight.

IV. RESULTS AND DISCUSSION

A. INTRODUCTION

All of the cases that were analyzed had some common relationships between them. The cases that happened along the Central Coast of California could be classified into the two distinct categories: dropping low (five cases) and frontal passage (11 cases). The frontal passage cases could further be subdivided into two separate categories of “fast moving fronts” and “extended gradients/stalling fronts.” There were seven “fast moving fronts” cases and four extended gradient cases.

Several features are common for all the selected cases. First, when the Monterey Airport has a southerly wind exceeded by 10 ms^{-1}, higher pressure was found at Buoy 28 compared to that at Buoy 42. Secondly, the increase of the southerly wind at the Salinas Airport seems to lag behind that southerly wind acceleration at Buoy 42. Finally, wind speed change at the Monterey Airport would be the last of the three wind speed measurements points (Buoy 42, Salinas Airport, and the Monterey Airport) to show an increase in wind speed.

B. SURFACE PRESSURE GRADIENT RELATIONSHIP

The pressure gradient relationship between the winds that occur at the Monterey Airport and the pressure difference between Buoy 28 and Buoy 42 should exhibit some skill in determining the strength in the wind speed gust at the Monterey Airport. The winds that occur along the Central Coast of California can show a blocked flow response (Doyle 1997). A blocked flow pattern will then lead to the presence of a barrier jet on the Central California coastline. The barrier jet response is dominated by a strong pressure gradient difference between two points that will cause it to be in an ageostrophic response while flow in a more unblocked pattern will go towards a geostrophic response. Thus, Buoy 42 winds should directly relate to the pressure difference between the Buoy 28 and Buoy 42 and the Monterey Airport would also relate to this same pattern

given the close proximity to Buoy 42. The response might not relate to the pressure difference between Buoy 28 and Buoy 42 if some effect in the lee of the topography limits the response of the winds to the pressure difference between the buoys.

All 16 cases display a tendency that the pressure gradient force between Buoys 28 and 42 is correlated with wind gust strength at the Monterey Airport. The results show that variance of the speed of the gusts at the Monterey Airport can be explained up to 90% by a simple linear relationship that has been derived from the pressure differences between buoys 42 and 28 (Figure 3 and Figure 4). Figure 3 was generated by taking the highest pressure difference between the Buoy 28 and Buoy 42, then comparing this difference with the highest wind speed gust that was recorded within 12 hours of the highest pressure difference. Figure 3 shows positive correlation where the higher the pressure difference between Buoy 28 and Buoy 42 the higher the wind speed gust potential.

Figure 4 displays the 16 cases and shows the actual pressure difference between Buoy 28 and Buoy 42. Figure 4 also shows the highest wind speed gust that took place at the Monterey Airport during each case. The last column shows the time difference between when the highest winds hit at the Monterey Airport and when the highest pressure difference occurred between Buoy 28 and Buoy 42. A positive value here corresponds to the highest pressure difference occurring before the highest wind speed gust at the Monterey Airport. The pressure difference technique is a now-forecasting technique to estimate the wind speed gust at the Monterey Airport.

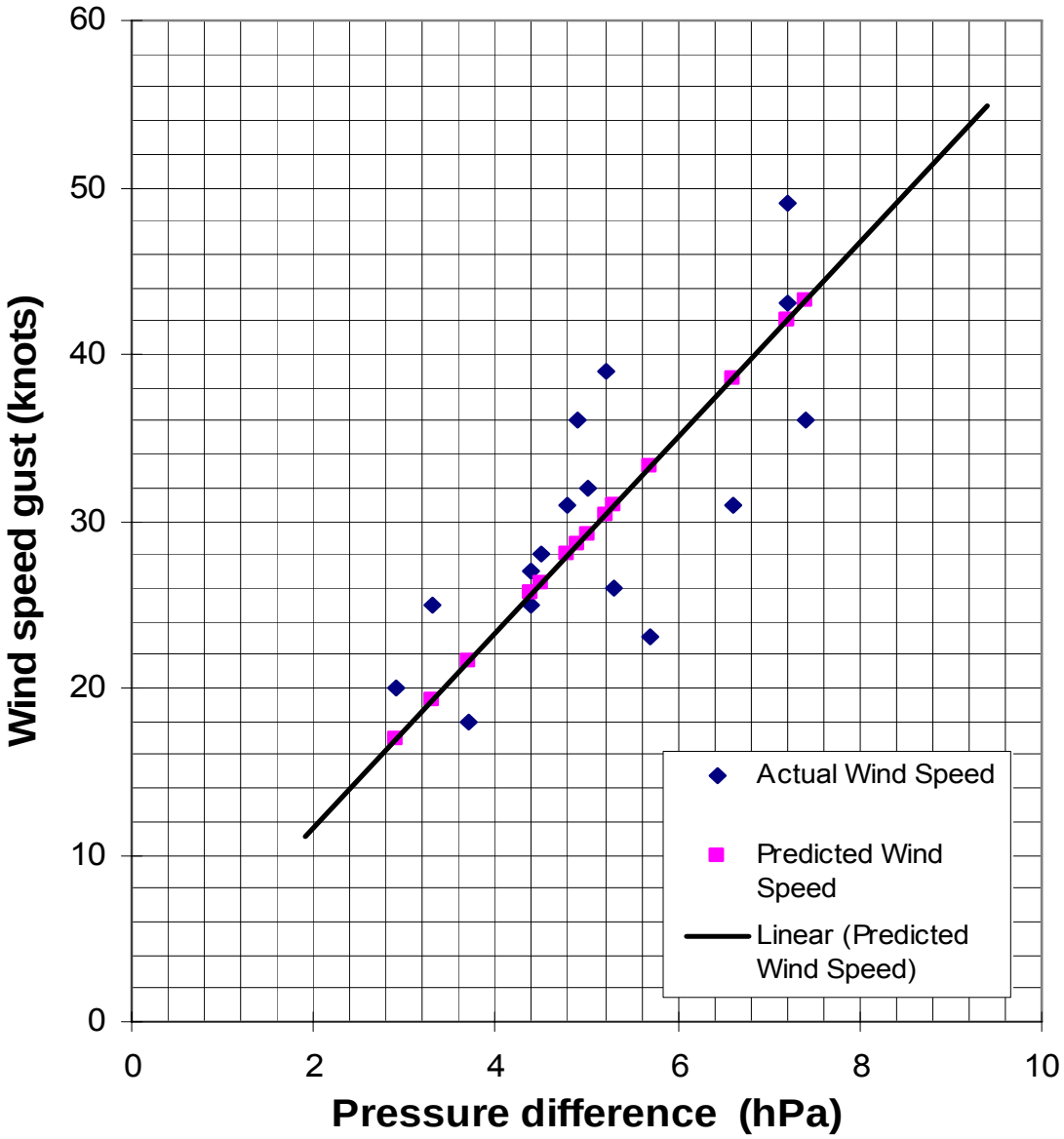

Figure 3. Correlation between wind gust speed, at the Monterey Airport, and pressure difference between Buoy 28 and Buoy 42. The error bars denote a 95% confidence interval as to the expected range of wind gust strength. The predicted wind speed line shows what the expected values for a wind gust given a SLP difference between Buoy 28 and Buoy 42.

Table 1. The columns are the following: case number on the left, next the surface pressure difference between Buoy 28 and Buoy 42 (ΔP), then highest observed wind speed gust, and last is the difference between the high-wind time at the Monterey Airport, and the time of highest SLP difference between Buoys 28 and 42. A positive time means that the highest SLP difference happened before the highest wind speed while a negative time means that the highest SLP difference happened after the highest wind speed at the Monterey Airport.

case #	ΔP (hPa)	High wind speed gust (kts)	ΔT (hrs)
1	5.7	23	-4
2	7.2	43	2
3	4.8	31	0.1
4	5.3	26	2
5	2.9	20	-4
6	3.3	25	0
7	4.2	30	1
8	7.4	36	2
9	4.9	36	0
10	4.4	25	-1
13	6.6	31	0
14	7.2	49	4
15	4.5	28	0
16	5	32	1
17	3.7	18	2
18	5.2	39	-3

These 16 cases show a clear trend between the wind speeds at the Monterey Airport and the surface pressure data at the two buoy locations. Such trend can be used as a diagnostic tool to 'nowcast' wind speed based on pressure difference at the two buoy locations (result of linear regression shown in Figure 3). For example if the pressure difference of 7 hPa was recorded between Buoy 28 and Buoy 42 one would expect a wind gust of 42 knots at the Monterey Airport.

C. RESULTS FROM EXAMPLE CASES

As noted in a previous chapter, three cases were examined in more detail in order to understand the temporal and spatial variability of the topographically influenced winds. An analysis of the Froude number, gap flow potential for the

Salinas Valley, as well as a synoptic and mesoscale analyses were done to characterize the wind variability over the region.

To examine the variation in winds at Monterey, the Froude number was calculated in order to characterize the degree of flow blocking. The Froude Number was calculated every three hours for all three cases. To calculate the Froude number, the 850 hPa wind was taken from the mesoscale reanalysis fields as well as the Brunt-Vaisala frequency (N) around the northern sections of the Santa Lucia Mountain range. The wind direction onto the northern sections of the Santa Lucia Mountain range would have a direction, normal to the mountain range if the direction is 240 degrees. To obtain the wind vector component normal to the Mountain range, in the Froude equation, the wind speed (U) is multiplied by the cosine (240-A), where A is the compass of the incoming wind in degrees. The average height of the Santa Lucia Mountain range was chosen to be H=1000 meters. These values were used to calculate the Froude number, as presented in Equation (1) (Table 2). N was computed from the model output of the mesoscale analysis. All three cases showed some interesting results which are explained in following sections

Table 2. The columns are divided into wind speed, wind direction, wind speed normal to the coastline at 850 hPa, Brunt-Vaisala frequency, and the calculated the Froude number Analysis for the three selected cases. Date and time of all three cases are also given in this table.

Date	Time	Actual Wind direction	Actual Wind speed (knots) @ 850 hPa	Wind component normal to land (ms^{-1})	Brunt-Vaisala Frequency-N (s^-1)	Froude Number (unitless)
4-Jan-08	0600Z	190	25	8.266	0.01095	0.75
4-Jan-08	0900Z	200	30	11.8226	0.01304	0.91
4-Jan-08	1200Z	210	30	13.3	0.01414	0.94
4-Jan-08	1500Z	240	40	20.57778	0.01449	1.42
4-Jan-08	1800Z	230	50	25.33144	0.01378	1.83
4-Jan-08	2100Z	240	55	28.29	0.01449	1.95
5-Jan-08	0000Z	250	40	20.26	0.01095	1.85
5-Jan-08	0300Z	260	25	12.089	0.01	1.21
5-Jan-08	0600Z	270	20	8.9	0.01	0.89
25-Jan-08	0600Z	200	15	5.9	0.01095	0.5388
25-Jan-08	0900Z	180	25	6.43	0.01095	0.5872
25-Jan-08	1200Z	180	35	9	0.0114	0.7895
25-Jan-08	1500Z	190	35	11.57	0.01095	1.0566
25-Jan-08	1800Z	180	45	11.57	0.010488	1.1031
25-Jan-08	2100Z	180	40	10.288	0.01	1.0288
26-Jan-08	0000Z	180	40	10.288	0.0114	0.90245
26-Jan-08	0300Z	180	50	12.86	0.010488	1.226
26-Jan-08	0600Z	180	50	12.86	0.01095	1.1744
26-Jan-08	0900Z	170	40	7.03	0.01095	0.642
26-Jan-08	1200Z	160	30	2.68	0.01	0.268
26-Jan-08	1500Z	170	40	7.03	0.0114	0.6167
26-Jan-08	1800Z	180	30	7.716	0.01183	0.6521
26-Jan-08	2100Z	170	25	4.399	0.01183	0.3719
27-Jan-08	0000Z	160	35	3.1266	0.01	0.31266
27-Jan-08	0300Z	160	30	2.68	0.01095	0.2447
27-Jan-08	0600Z	160	40	3.57	0.011832	0.3017
27-Jan-08	0900Z	170	55	9.7	0.014142	0.6859
27-Jan-08	1200Z	180	30	7.7	0.0114	0.6753
27-Jan-08	1500Z	190	20	6.61	0.01095	0.60397
27-Jan-08	1800Z	200	25	9.85	0.011832	0.83267
27-Jan-08	2100Z	230	20	10.13	0.011832	0.856
28-Jan-08	0000Z	220	25	12.085	0.01	1.2085
28-Jan-08	0300Z	240	20	10.2888	0.01095	0.94
23-Feb-08	1800Z	200	25	9.8521	0.015492	0.6351
23-Feb-08	2100Z	210	45	20	0.01732	1.1547
24-Feb-08	0000Z	190	50	16.5339	0.014142	1.1691
24-Feb-08	0300Z	220	35	16.919	0.01265	1.3376
24-Feb-08	0600Z	240	30	15.433	0.01095	1.4094
24-Feb-08	0900Z	240	25	12.86	0.009486	1.35556
24-Feb-08	1200Z	230	20	10.13	0.009486	1.06816
24-Feb-08	1500Z	260	35	16.9197	0.010488	1.613
24-Feb-08	1800Z	270	30	13.365	0.01095	1.22
24-Feb-08	2100Z	280	20	7.78	0.01	0.788
25-Feb-08	0000Z	270	15	6.6828	0.01	0.66828

To determine the contributions of gap flow forcing to high winds at the Salinas Airport, the Salinas to Paso Robles pressure difference was calculated to correlate with the wind speed gust at the Salinas Airport. If high winds occur at the Salinas Airport, then analyzing the SLP difference between two locations in the Salinas Valley would predict this behavior as theory would indicate (Mass et al. 1995). The Salinas Airport and the Paso Robles Airports were used as reference points for estimating the speed of the wind speed gust at the Salinas Airport. The strong winds from the southeast would need to have a pressure higher at the Paso Robles Airport than the Salinas Airport. This coincides with the fact that winds blow on land from high pressure to low pressure; especially in channeled flow (Mass et al. 1995).

Figure 4 shows how the wind speed at the Salinas airport is correlated to the pressure difference between the Paso Robles airport and the Salinas airport. Figure 4 also shows that the higher the pressure difference between Paso Robles airport and the Salinas airport will lead to a higher wind speed at the Salinas airport. However, such correlation is only seen if the Paso Robles airport is at least 2 hPa higher than the Salinas airport in surface pressure. Following a linear regression relationship of the two quantities, it is determinable that if the pressure between the Paso Robles airport and the Salinas airport were 4 hPa, the wind speed gust would be equal to 34.7 knots. Table 3 displays the regression statistics for Figure 4.

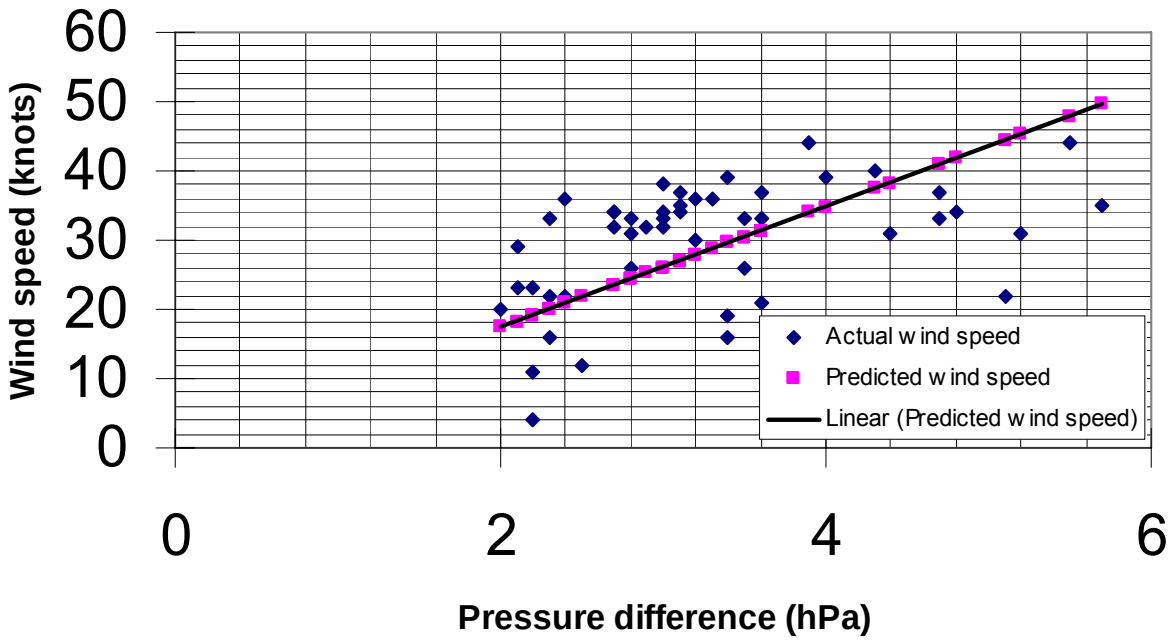

Figure 4. Wind speed gust at the Salinas Airport, from the pressure difference between the Salinas Airport and the Paso Robles Airport, correlates with wind speed gust (measured in knots) at the Salinas Airport.

Table 3. Regression statistics for measured speed and calculated (from pressure gradient) speed. Data are from the Paso Robles and Salinas Airports calculation.

Regression Statistics	
Multiple R	0.957442
R Square	0.916696
Adjusted R Square	0.895419
Standard Error	9.05597
Observations	48

The regression analysis shows 89% of the variance in the strength of the wind speed gust for a tolerance of 95%, predicts the wind speed within +/- 9 knots (so an 18-knot wind range). The winds can be predicted using a "now-casting" forecast technique to estimate the wind strength in the Salinas valley for the Salinas Airport but the spread has a higher spread than what was seen for the Monterey Airport wind speed gust. One reason that contributes to the large wind speed range is that only three cases worth of data were used to construct this model. In addition, the start of the Salinas Valley does not start in the city of Paso Robles but begins 30 miles to the north of Paso Robles which would help give a better pressure difference to predict how strong the winds could be at the Salinas Airport as theory would suggest (Mass et al. 1995). The flow might be parallel in one of the three cases but in another case, it might have been perpendicular which would cause the winds to either accelerate or decelerate through the Salinas Valley depending upon the pressure gradient orientation.

1. Case 1 (January 3-5, 2008)

a. Synoptic Overview

This damaging weather event occurred along the northern two-thirds of California coastal areas, the Oregon coast, and extended into southern reaches of the Washington coastline. There were, at one time during the height of the storm 1.2 million customers without power and wind gusts were as high as 80mph in some lower lying areas (*January 2008 Western North American Super Storm*). The initial setup of the storm had an upper level ridge centered over the mountain west region of the United States on January 2, with an upper level trough over the Eastern Pacific Ocean.

Over the next three days, the upper level pattern stays intact. The Polar Frontal Jet (PFJ) at 500 hPa had a jet maximum jet speed around 145 knots at 0000Z on January 4. The jet streak was located around 46N and 145W and helped to rapidly intensify the weather system that made landfall along the Western United States over the next 12-24 hours. By 0000Z on January 4 the

low had deepened to 960hPa and at 1200Z continued to deepen to roughly a 958hPa (Figure 5 and Figure 6). The pressure gradient over the Central California coastline started to become tighter as the low pressure over the North Eastern Pacific Ocean moves closer to the North American coastline. The closer (or tighter) the isobars get to one another the faster the wind speed will be around the low-pressure center. As the winds begin to pickup along the Central California coastline, the topography will block the cross-shore component of the wind and disrupt geostrophic balance as what was previously found out in Doyle (1997). With the flow blocking a barrier jet will form along the Central California coastline.

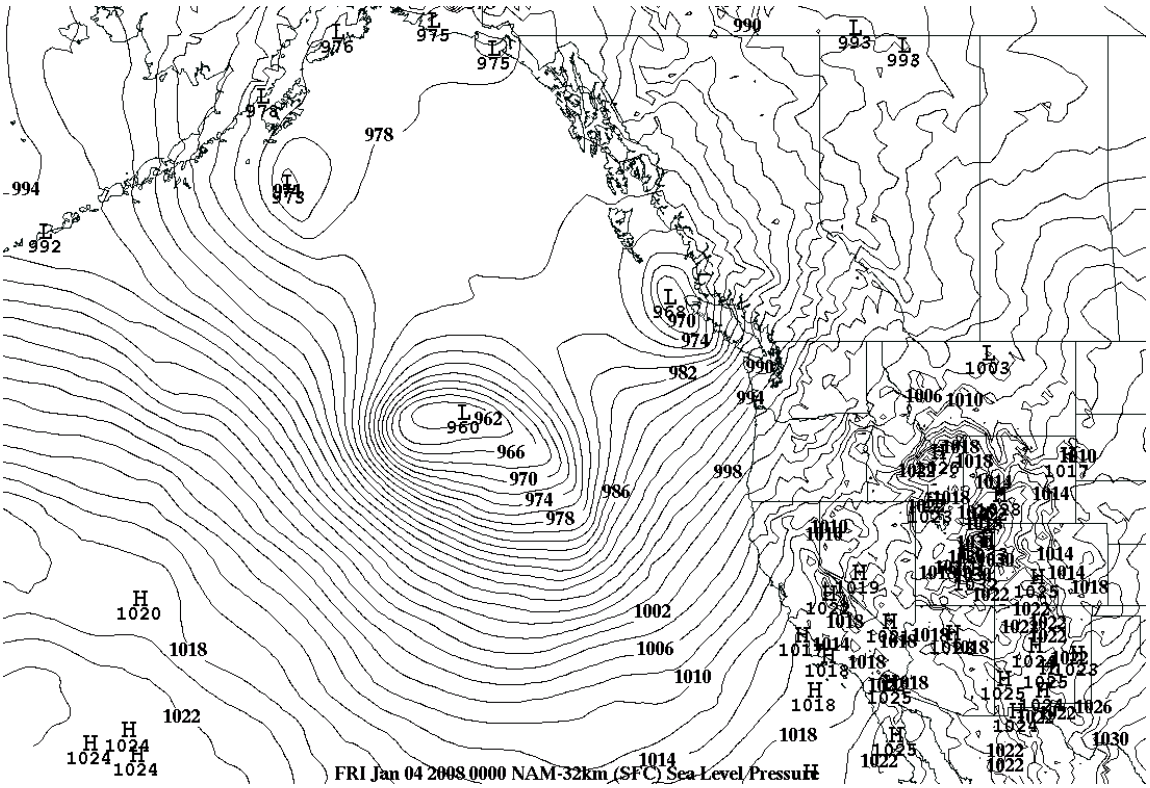

Figure 5. Storm location at 0000Z on January 4. Contour labels are in pressure in hPa.

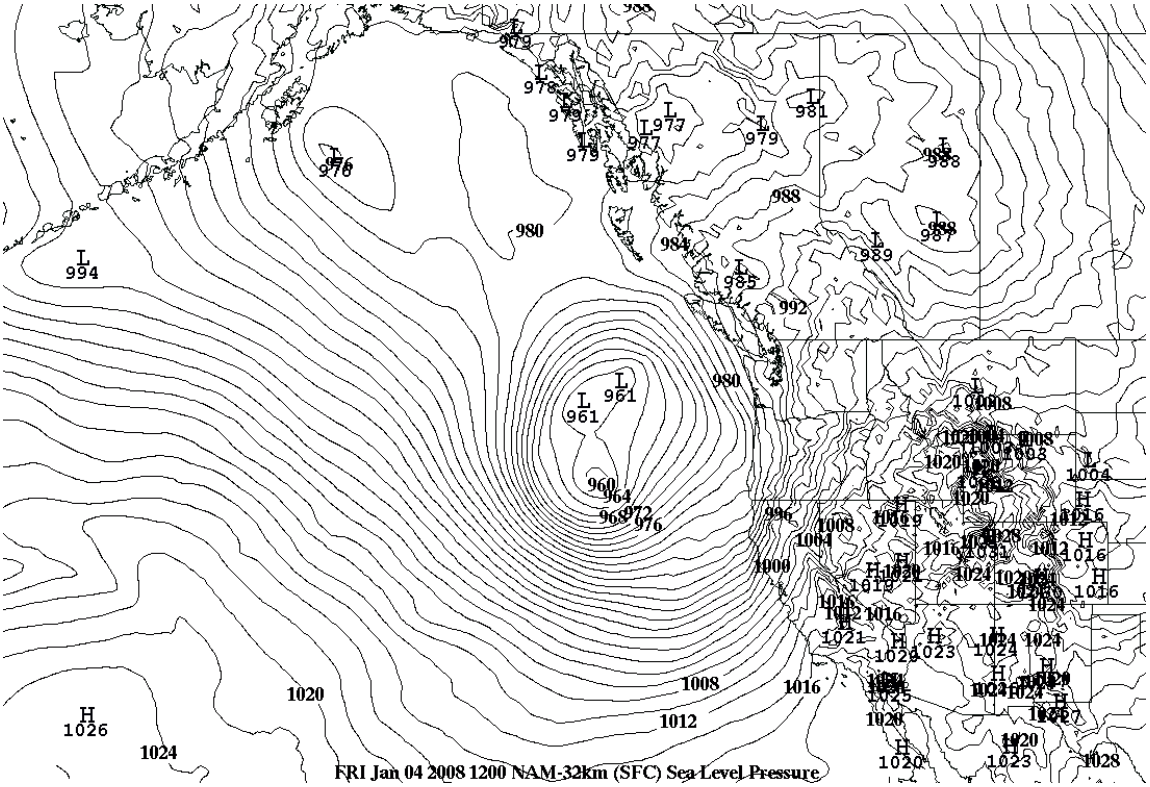

Figure 6. The storm location at 1200Z on January 4.

By 0000Z, on January 5, the storm had deepened to its lowest level of 957hPa and it was located about 200 miles off the coast of Vancouver Island Canada (Lewitsky). The strongest low level winds were felt along coastal locations as well as Sierra Ridgelines where the coastal location gusts were reported as high as 80mph while in the Sierras wind speed gusts were reported as high as 160 mph (January 2008 Western North American Super Storm).

The system fit the land falling frontal category, i.e., the associated low pressure center continued to move away from the Central California coastline towards Vancouver Island and a front, which can be seen on the 0600Z and 1800Z satellite images on January 4, approached the coastline (Figure 7 and Figure 8).

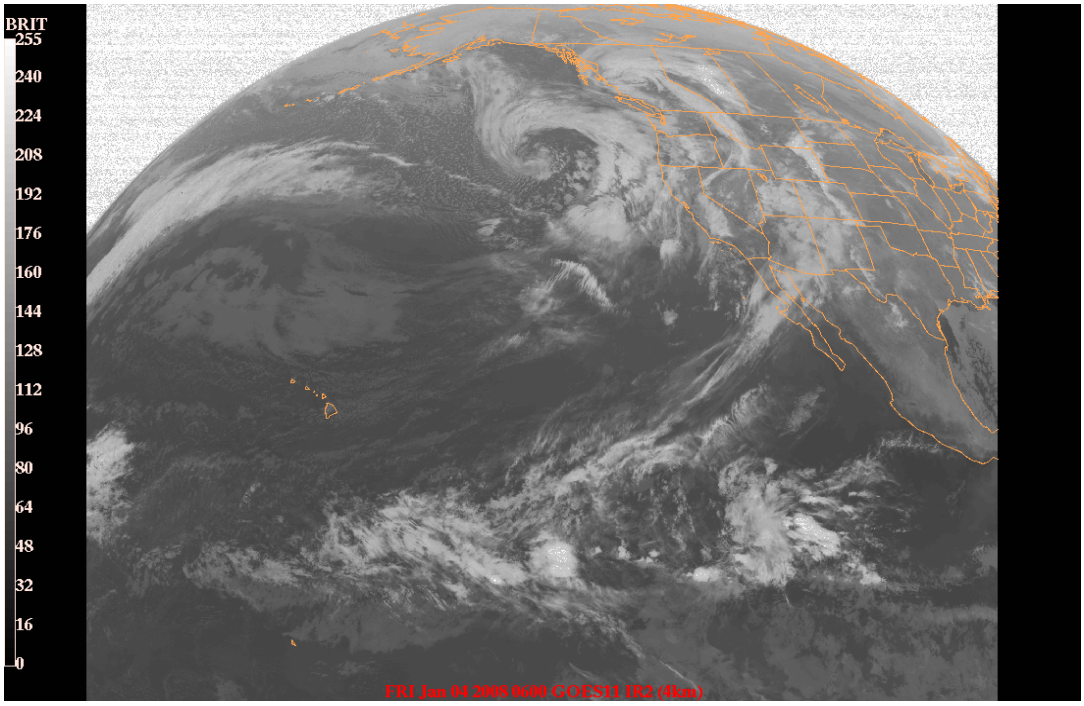

Figure 7. Infrared Image of the storm as it approaches California on January 4 at 0600Z.

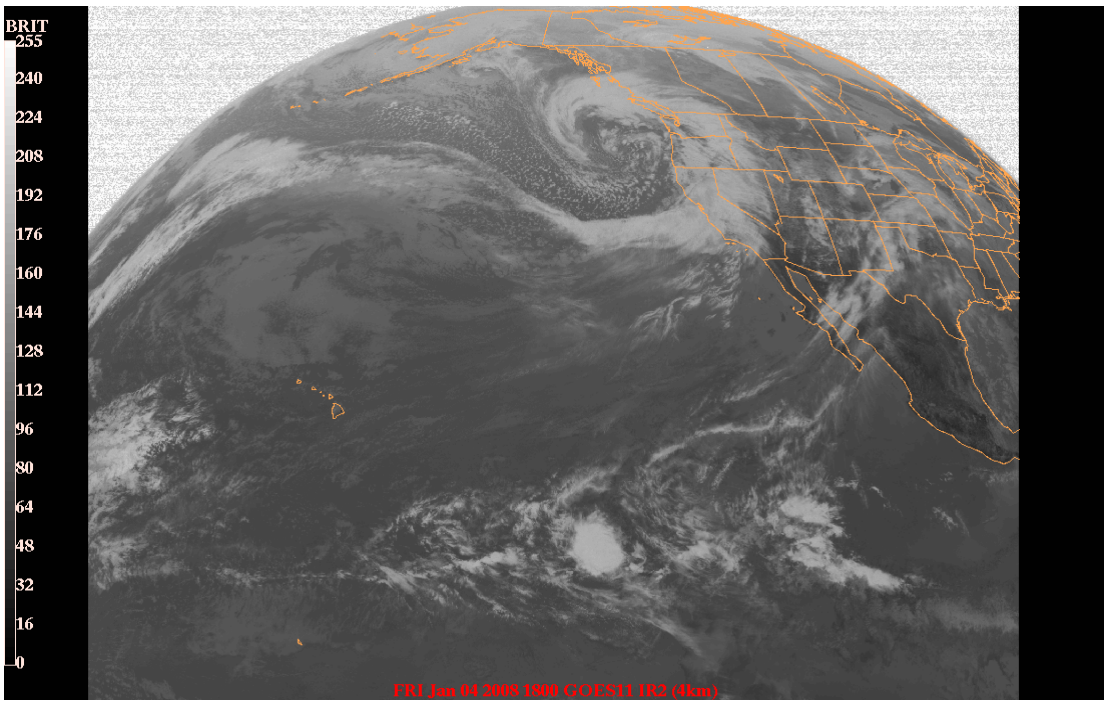

Figure 8. Infrared Image of the storm at 1800Z as it approaches California on January 4.

b. Mesoscale Effects Around the Monterey Peninsula Region

Wind speeds during the event actually show that the winds at Buoy 42, on January 2 begin the day as very light and variable but by the end of the day winds are now blowing from the south-southeast direction at around 10 knots. The winds continue to gain in strength over the next day so that on January 4 at 0000Z the winds are gusting to strength of around 30 knots from the south-southeast with sustained wind speeds around 25 knots. The winds, on January 4, continued to gain strength over the day until they reach a maximum of 21.5 ms^{-1} (43 knots) at 1400Z; however, the winds continued to blow at speeds over 40 knots in strength from the SE until 1900Z on January 4. There is a substantial shift in the wind speed and direction. The winds decrease in speed to fewer than 20 knots and the direction of the wind changes to a southwesterly direction by 0000Z on January 5, which-corresponds with frontal passage in the region.

The observations at the Monterey Airport show a different trend leading up to the time of maximum winds. Early on January 3 the winds are light and variable with some upper level cirrus clouds overhead that is coming from the weather system that will affect the Monterey Airport the next day. The clouds begin to thicken up and the temperatures rise between 0600Z and 2100Z on January 3. Also the pressure mainly shows a decreasing trend on January 3 as the weather system approaches the Monterey Airport. The pressure actually begins to rise on January 4 around 0400Z, but by 0600Z the pressure begins to drop very rapidly as the weather system front begins to bear down on the Monterey Airport. January 4 sees the winds begin to increase in speed over the Monterey Airport starting around 1200Z; however, before 1200Z the winds were calm at Monterey Airport at 0700Z (the calm before the storm). The winds continue to increase in speed to a maximum of 49 knots recorded at 2235Z on January 4 with frontal passage. The time with highest winds also was the time

when a mesoscale low formed in the Monterey Bay (Figure 9 and Figure 10) as determined from the mesoscale reanalysis technique using the MADIS observations.

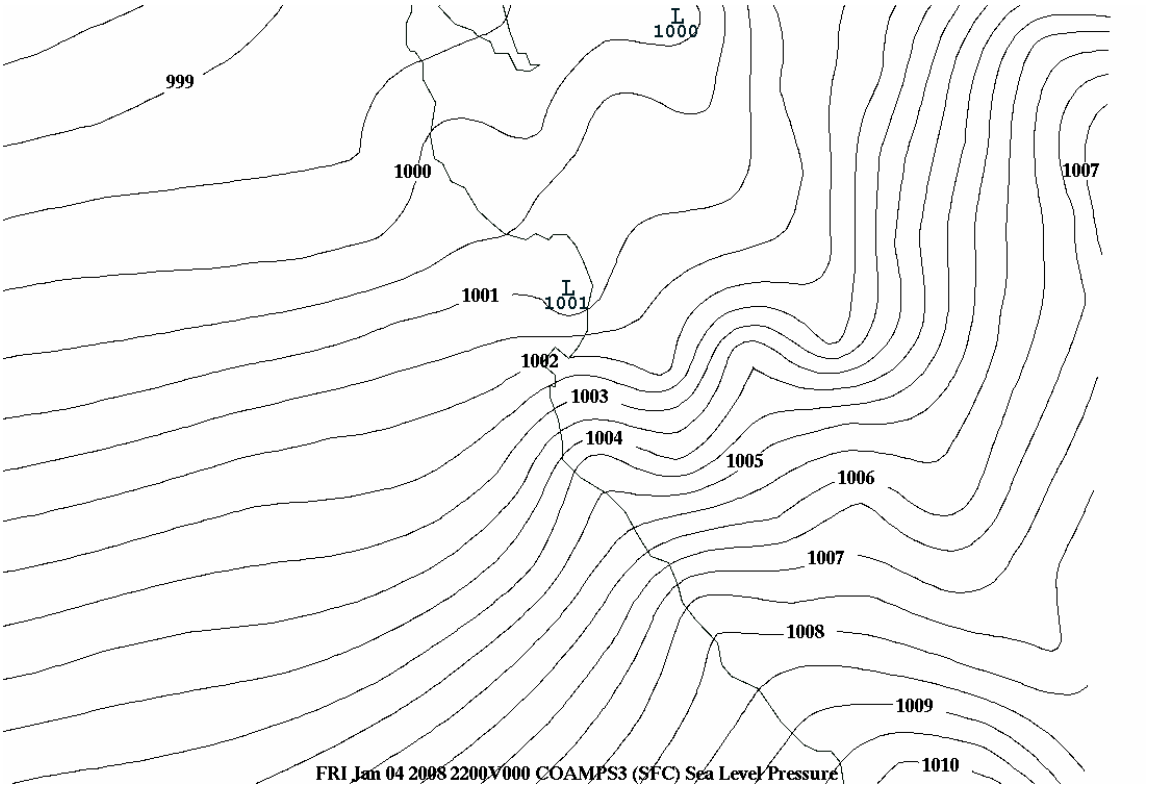

Figure 9. Mesoscale low pressure center in the Monterey Bay region at 2200Z on January 4.

The wind direction at the Monterey Airport is from the southeast starting from 1200Z in the morning and continues to be from the southeast until a cold front passage that takes place between 2200Z-2300Z. After this time, the winds blow from the southwest until 0800Z on January 5, when they finally become light and variable again.

The Salinas Airport and the Monterey Airport winds showed the same tendency on January 3. On January 4, the winds showed the same pattern that Monterey displayed, that is, the winds were from the southeast and

increased during the day. However, the fastest wind speeds that happened at Salinas actually occurred in the early morning hours when the wind blew at 39 knots from the southeast at 1200Z. The winds blew in the mid to upper 30s until 2000Z on January 4. The reason the winds blew sooner and less at the Salinas Airport versus the Monterey Airport is that gap flow effects probably contributed to the winds at the Salinas Airport. The pressure gradient in the Salinas Valley had a better alignment with the storm pattern in the early hours of the storm versus the later hours on January 4 (or near 0000Z 5 January as shown in Figure 11). The pressure gradient is highly aligned with the Salinas Valley as shown in Figure 10 but the pattern rotates to a more cross-valley direction by 0000Z on 5 January. On January 5, any gap flow forcing drops to near zero by this time.

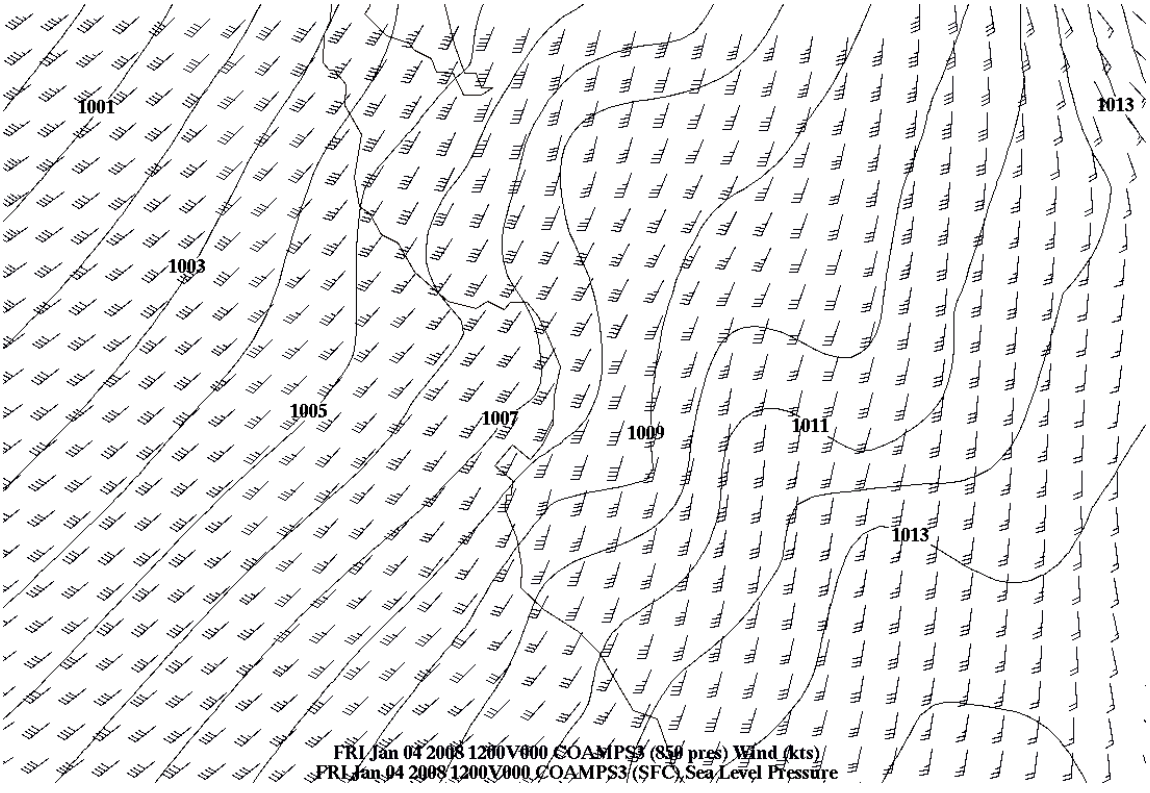

Figure 10. At 1200Z on January 4, the winds were strongest at the Salinas Airport with the winds at 850 hPa showing a strong southerly component.

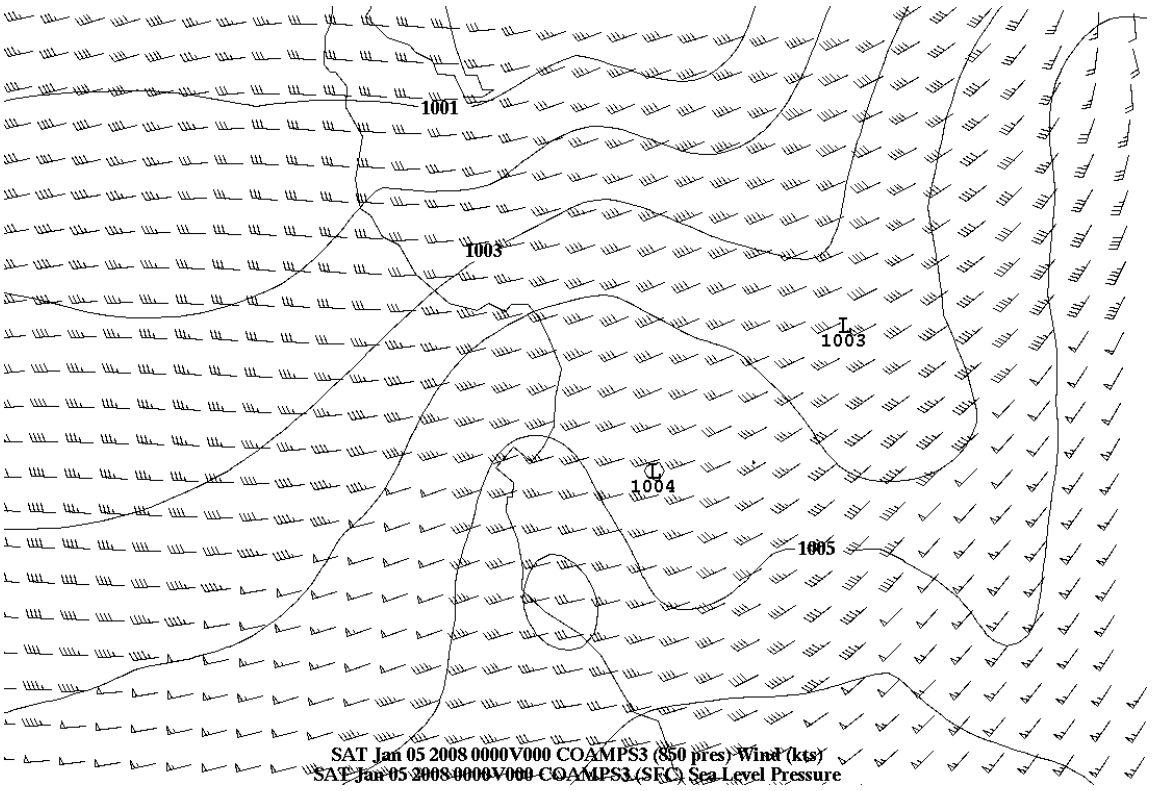

Figure 11. Calculation shows that the winds along with SLP field, at 0000Z on January 5, have a westerly component to them.

When winds along the Big Sur coastline are blocked by the coastal terrain, buoy observations show southeast wind direction, which is almost parallel with the coastline. Buoy 42 reports a wind gust of 19.2 ms^{-1} (37 knots) at 0300Z on January 4. The flow blockage produces a prefrontal barrier jet along the coastline on January 4 around 0600Z. This is consistent with the Froude number being less than unity from January 4 at 0000Z until 1300Z. The barrier jet can be verified by the fact that the wind speed gusts at Buoy 42 were in excess of 35 knots at 0300Z on 4 January. The flow is initially blocked. However, at 1300Z, it becomes “unblocked” and the barrier jet is no longer prevalent. The barrier jet did not go away but the sustained wind speeds and gusts seen at Buoy 42 were also the same in intensity and time as those winds seen at the Monterey airport from 1300Z on 4 January through the end of the high winds period at 0400Z on 5 January. This is consistent with the Froude number at 1200Z of approximately

0.94, which increased to well above unity after that time. By 1300Z, the flow is allowed to move over the mountain range and the winds show dramatic increase at the Monterey airport: changing from 6 knots at 1100Z to at least 21 knots by 1400Z with a southerly direction.

2. Case 2 (January 25-28, 2008)

a. Introduction

Case 2 was a dropping low event and wind evolution in the Monterey Bay region was different from the land falling frontal system examined in case 1. While winds along the coast at Buoy 42 were strong, the Monterey airport had much weaker winds throughout this case. In addition, winds at the Monterey airport tended to be easterly instead of southerly, suggesting a different type of topographic interaction.

b. Synoptic Overview

The storm in this case developed with support from upper-level northerly flow along the Eastern edge of the Pacific Ocean. A high-amplitude ridge was situated over the state of Alaska. There was longwave trough that covered the entire western United States. On January 24 at 0000Z, a shortwave trough (at 500 hPa) with a weak low at the surface associated with the trough started to move southeasterly along the coastline of North America (Figure 12).

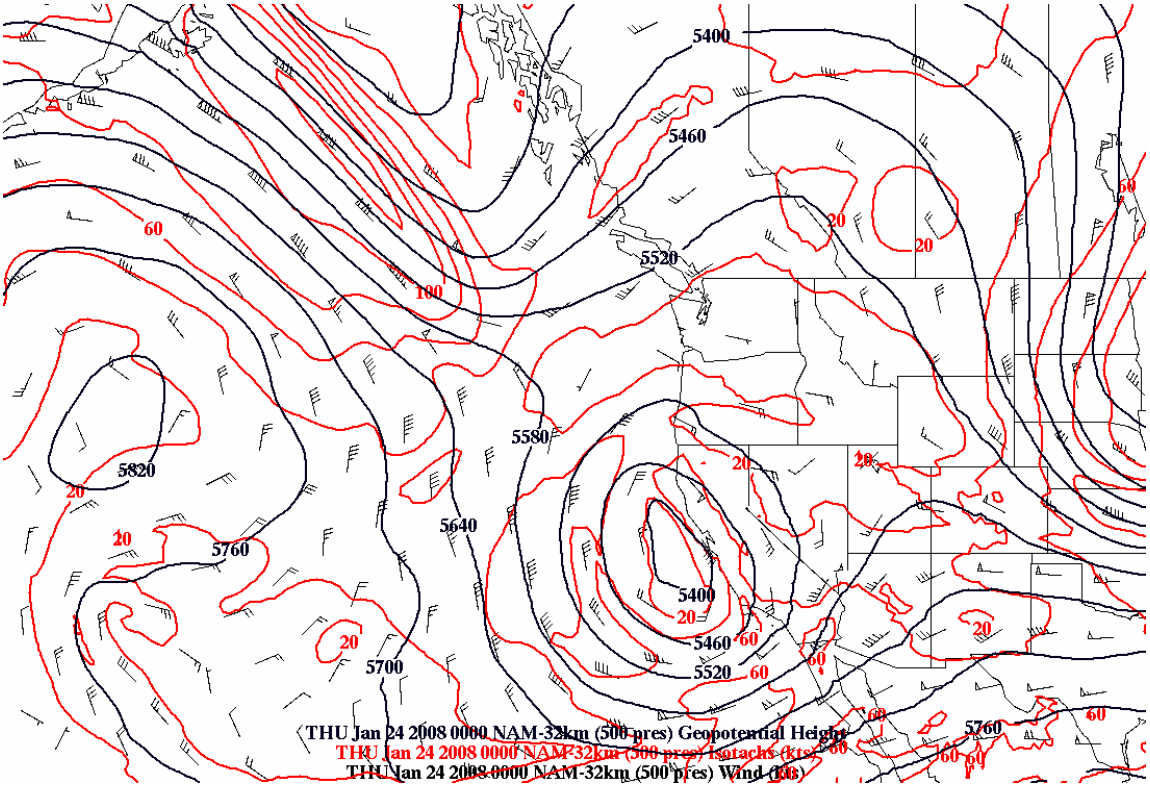

Figure 12. Display of an upper level trough, in the Gulf of Alaska, which has a 120 knot jet associated with it. A cut-off low is currently right off the central coast of California on January 24 at 0000Z. The red lines are isotachs and the black lines are height contours at 500hPa.

On January 24 at 1200Z, the surface low had a central pressure of 1003 hPa and it was located near the western edge of Vancouver Island. The upper-level trough was, at that time, an upper level low and the upper-level ridge did not change position during the next 12 hours. By 0000Z on January 25, the upper level ridge started moving more to the east by about 300 Nautical Miles. The upper-level low and surface low paralleled the North American coastline and were located west of the Oregon-California border in the Pacific Ocean. The surface low had a central pressure of 998 hPa. The Central California coastline was not seeing any significant winds or rains at this point (Figure 13).

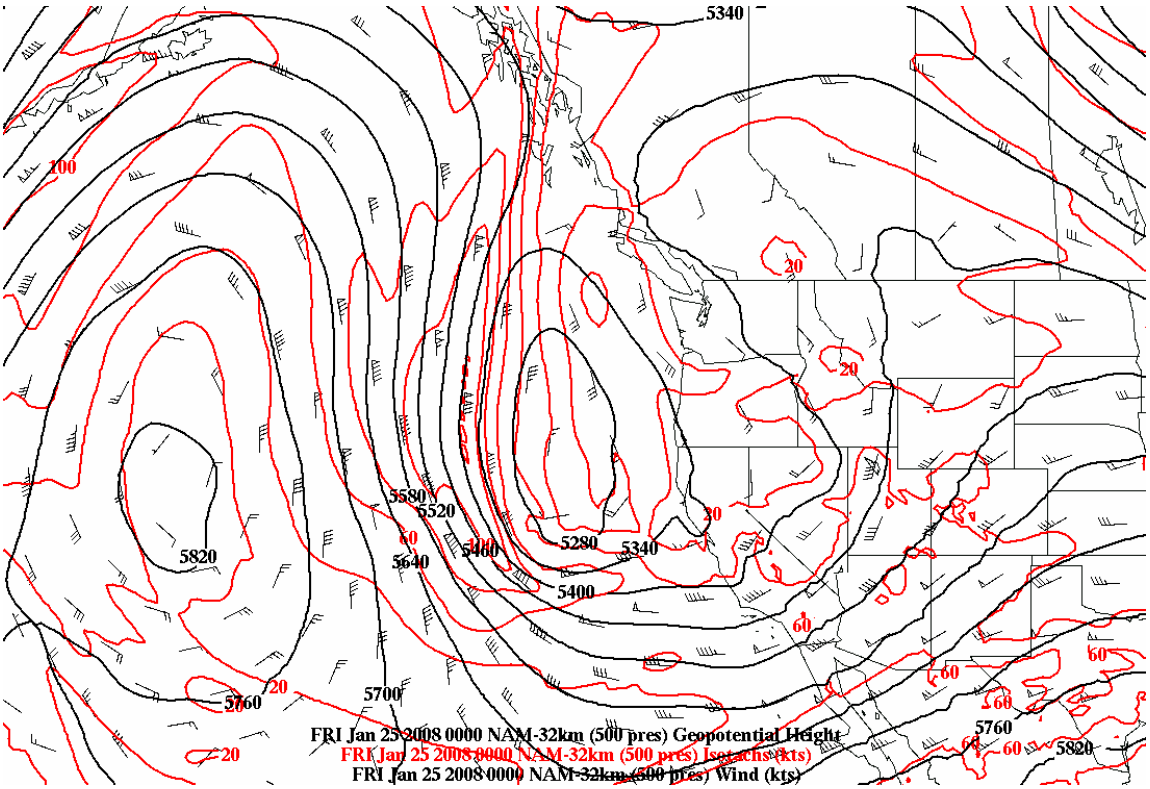

Figure 13. The upper level trough is now an upper level low with a 120 knot jet moving along the western side of the upper low.

On January 25 at 1200Z, the low had deepened to a central pressure of 995hPa and it was located west of San Francisco by about 280 Nautical miles. Also at this time, the low became barotropic with the upper-level low and the surface low being vertically stacked over the Pacific Ocean. Between 0000Z and 1200Z on January 25, the pressure gradient in the region became stronger (with the pressure being generally higher over land than over water) producing a strong offshore component to the winds (Figure 14). This east-west pressure gradient results in little along-coast gradient and therefore limits the degree of ageostrophic acceleration that might occur in a barrier jet.

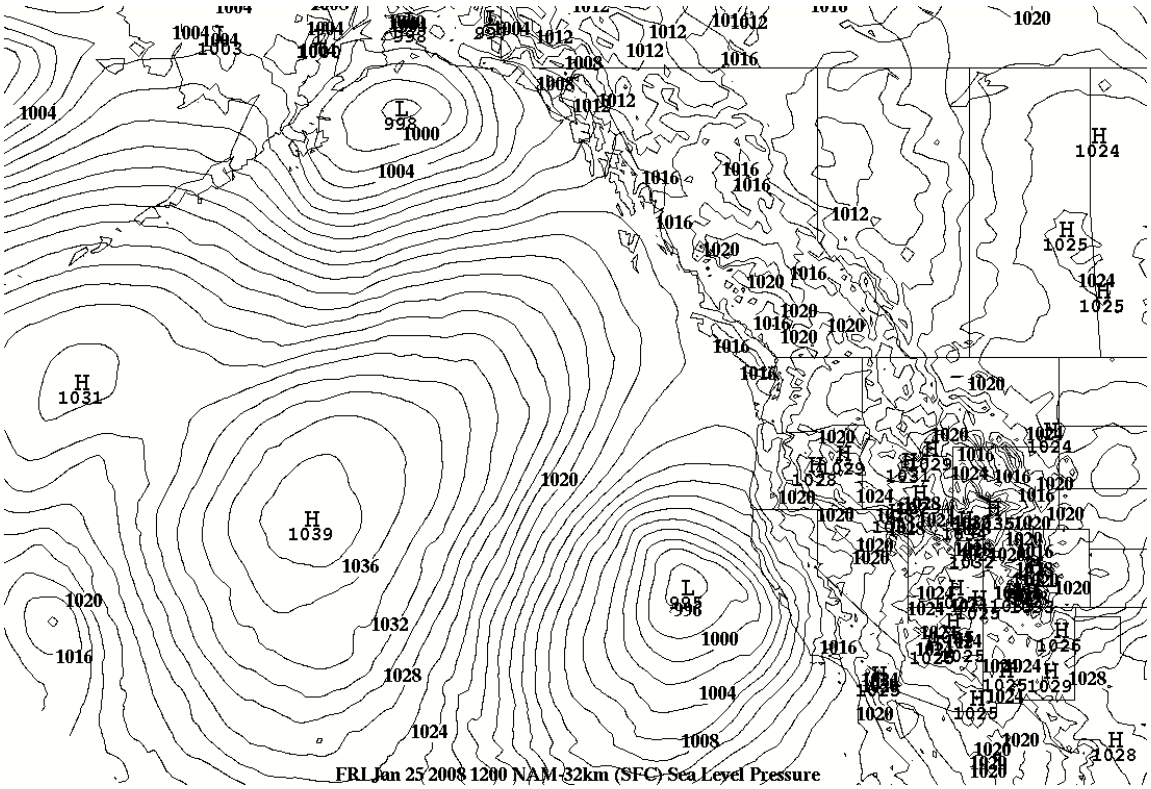

Figure 14. A low-pressure center value of 995 hPa centered west of California.

The next 12 hours shows that the low started to weaken and drift southward weakening the pressure gradient near the Central California coast. However, several small scale low pressure centers developed in the region helping to produce more mesoscale pressure gradients (Figure 15 and Figure 16), which can be seen on the surface chart.

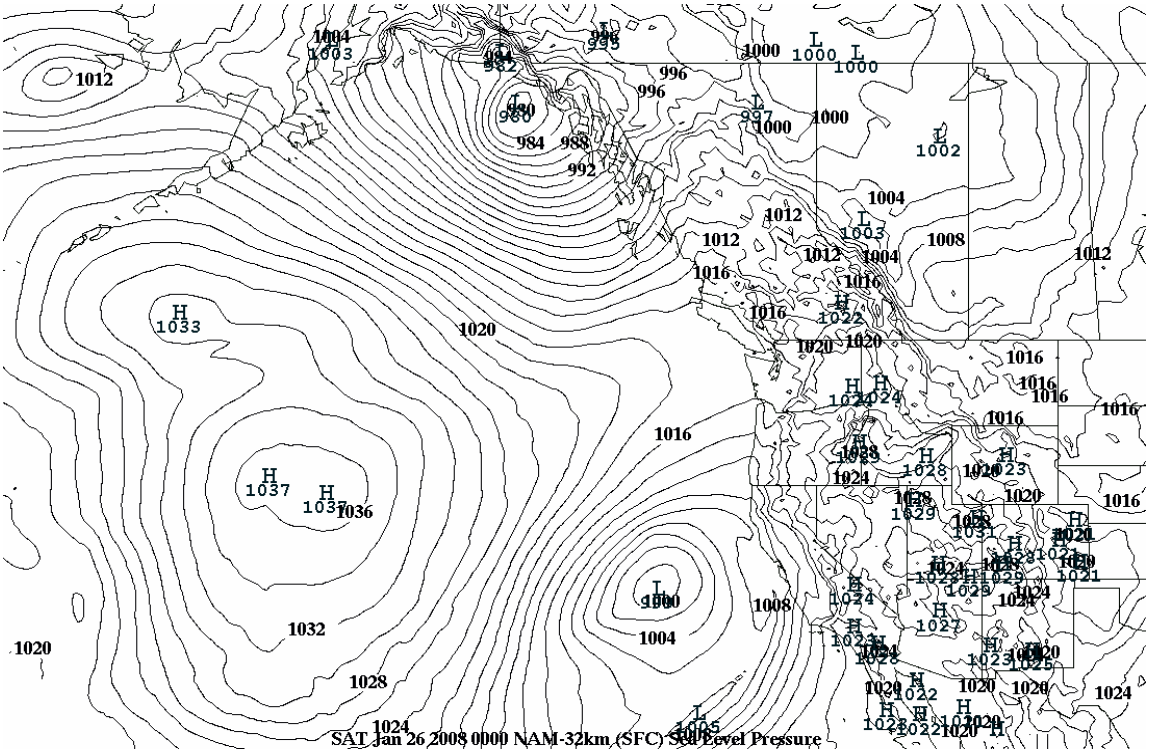

Figure 15. The SLP pattern on January 26 at 0000Z.

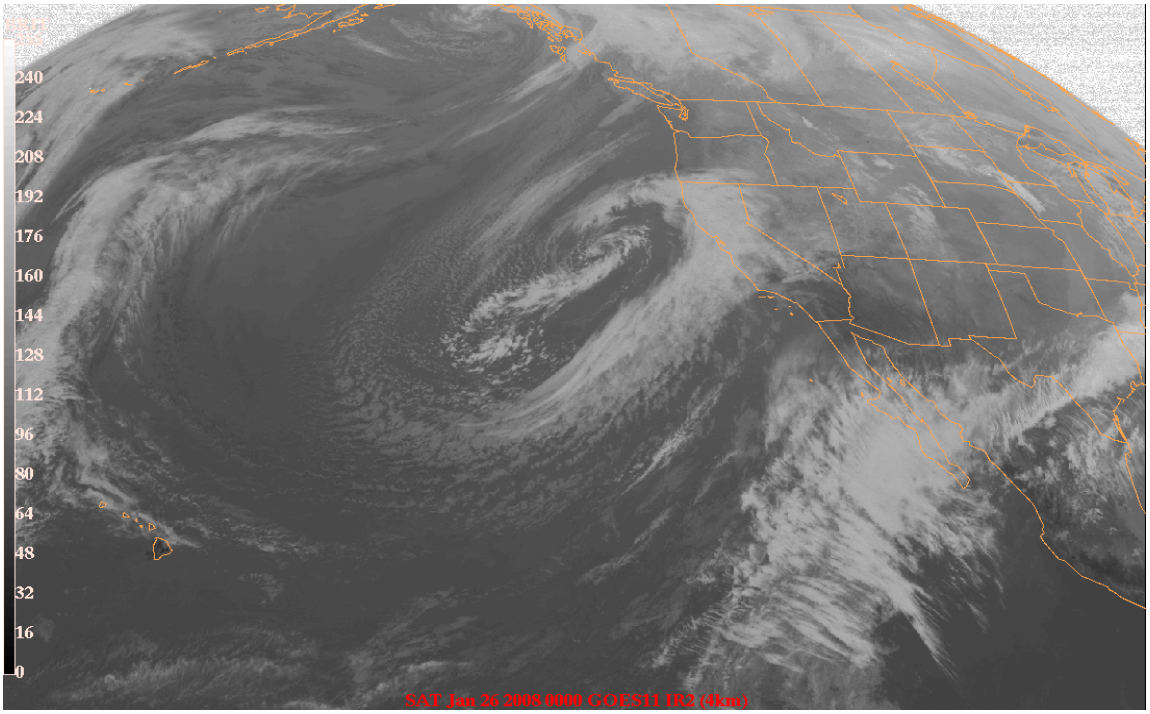

Figure 16. IR satellite image valid at 0000Z on January 26.

The parent low had filled to a central pressure of 999hPa, but small-scale lows were developing in the southern periphery of the low pressure center on January 26 at 0000Z. In addition, the upper level low had heights around 5330 meters at the lowest point right off the coast of California. However, the synoptic scale pressure gradient increased and helped to produce winds that were stronger than those during the preceding 12 hours along the Central California coastline. The winds were in excess of 40 knots at Buoy 42, while the Monterey Airport was seeing winds only as high as 18 knots. By January 26 at 1200Z, the low had continued to fill and had a central pressure of 1003 hPa. Some other secondary lows were forming to the south and east of the parent low, which was situated 550 nautical miles due west of Vandenberg AFB. At 0000Z on January 27, the low had a central pressure around 1003hPa, but a secondary low was forming and was 200 nautical miles to the northeast of the parent low (Figure 17 and Figure 18) resulting in a well defined cross coast pressure gradient and relative strong coastal winds.

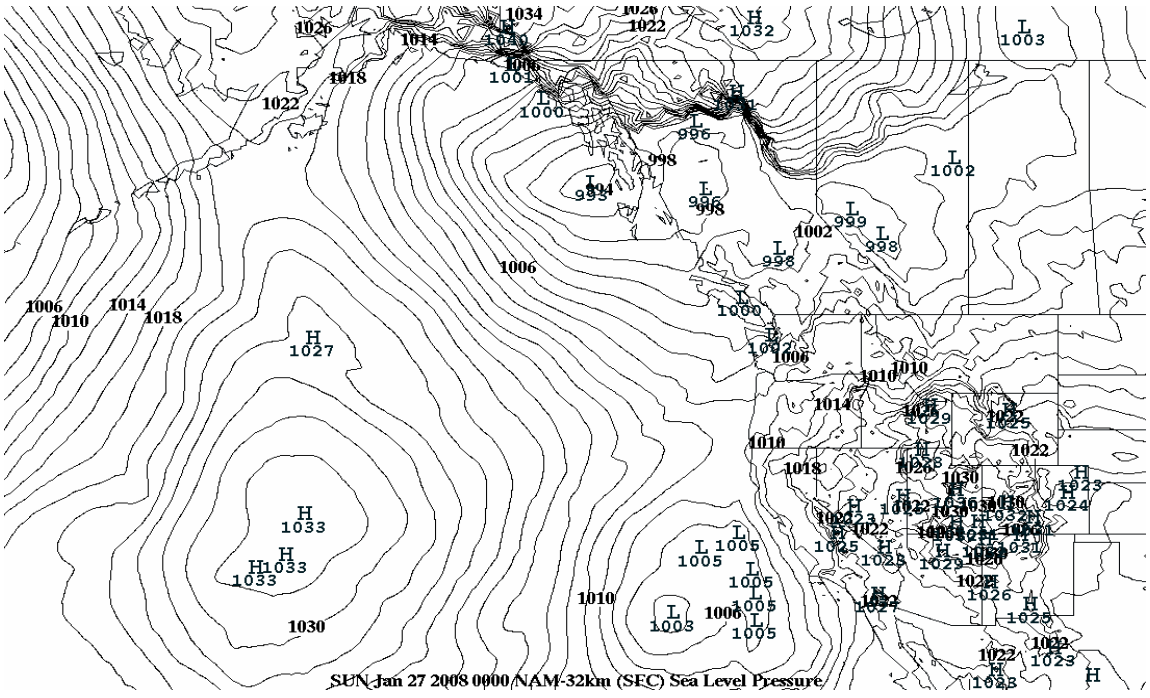

Figure 17. Multiple low centers in the Pacific Ocean off the coast of California on January 27 at 0000Z.

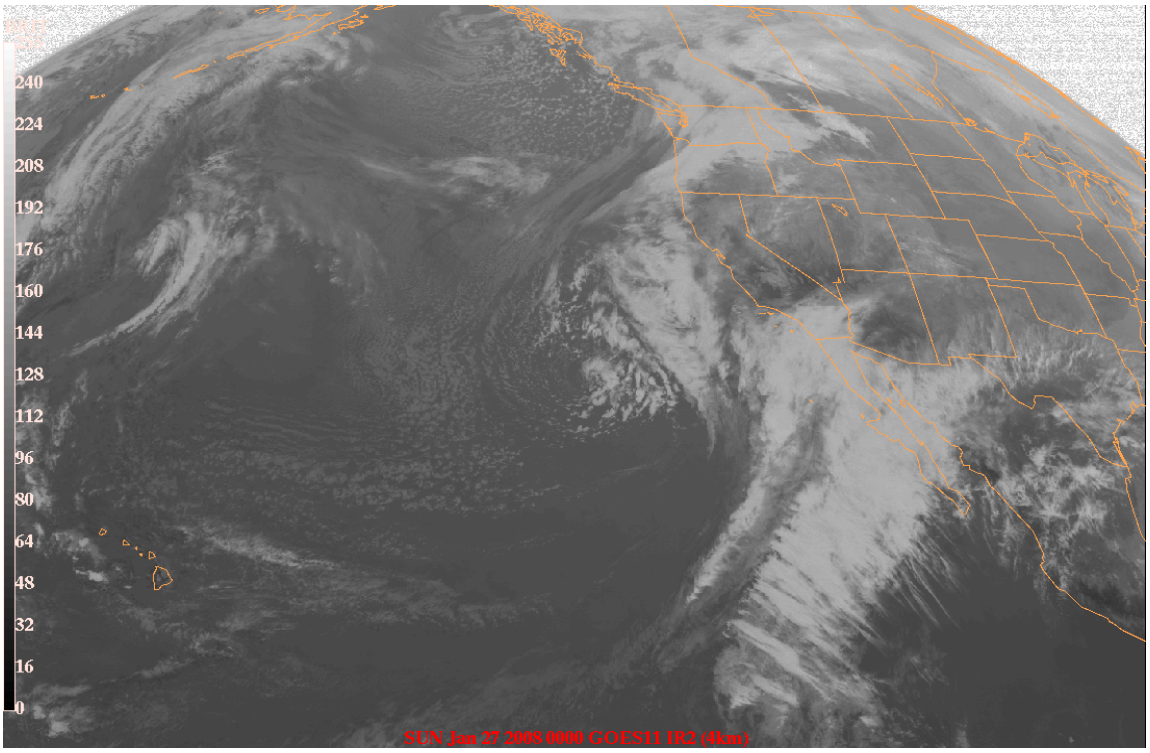

Figure 18. The IR satellite imagery for January 27 at 0000Z.

By 1200Z on January 27, the secondary low became the dominant low with a central pressure of 994hPa, and it helped to increase the pressure gradient in the Central California coastal region. The orientation of the pressure field changed where the flow would now have a more onshore component versus a more parallel component. The new low moved east over the next 12 hours and moved ashore by 0000Z on January 28 making landfall around Cape Mendocino (Figure 19) to produce a more definitive along-coast pressure gradient in the post-trough environment. Once the low moved further north, the pressure gradient became unfavorable for the production of strong southerly winds. The low weakened even more as it moved into Northern California (Figure 19 and Figure 20).

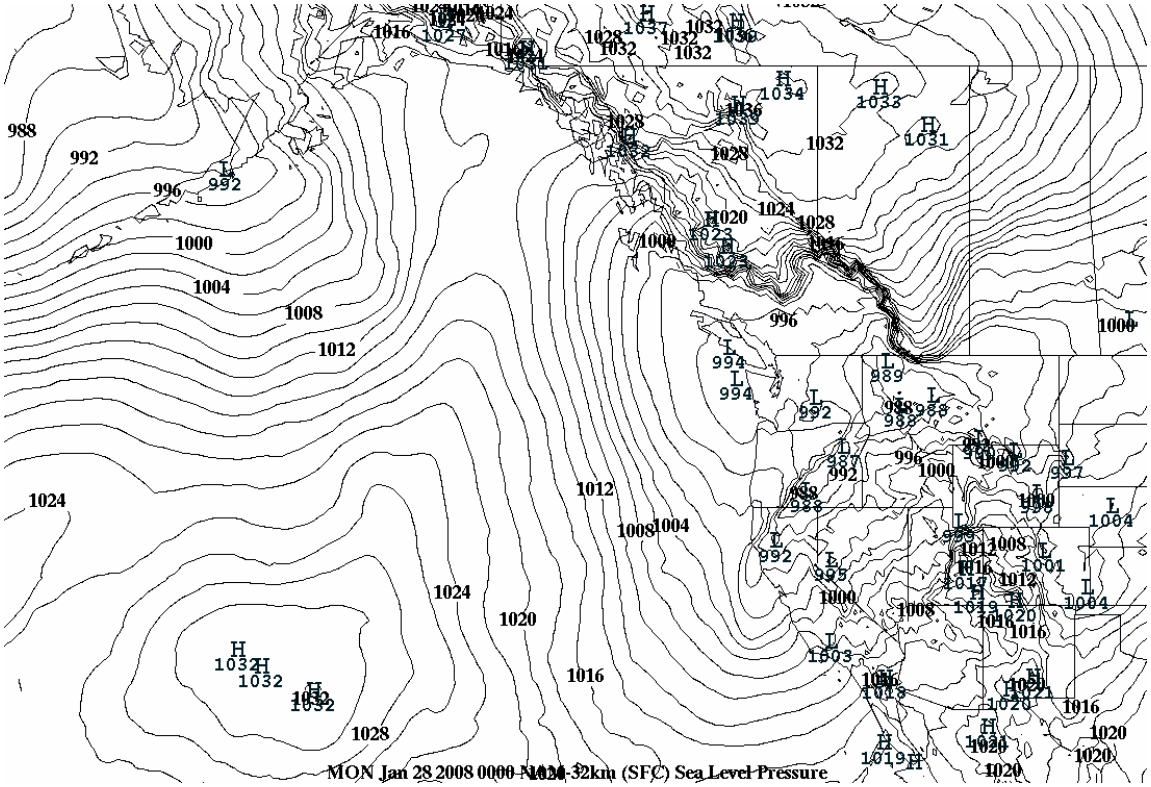

Figure 19. Surface low, making landfall in California, begins to fill rapidly at 0000Z on January 28.

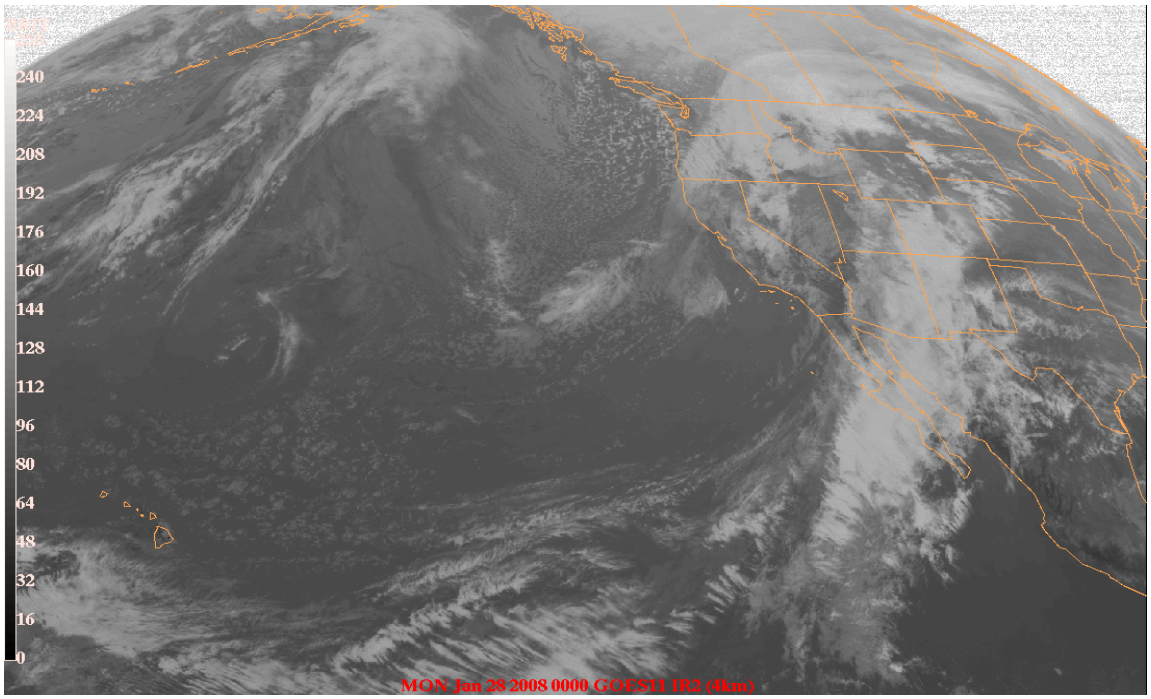

Figure 20. Satellite imagery for January 28 at 0000Z.

c. Mesoscale Effects Around the Monterey Peninsula Region

The winds at Buoy 42 start blowing on January 25 at 0000Z, from the south at speeds of 7-10 ms^{-1}. The winds continue to increase in strength, at Buoy 42, through the day on January 25 until the wind strength settles at a wind speed around 15-20 ms^{-1}. The maximum wind speed happens at 1700Z on January 25. High winds at Buoy 42 do not coincide with the flow being "blocked" as the Froude number was greater than unity. The wind speed gust at Buoy 42 was 25.4 ms^{-1} (49.2 knots) at 1700Z. However, at this same time the wind speed at the Monterey Airport was calm, which suggests that the wind was "blocked." The wind speed aloft decreases for the next 12 hours but the wind speeds at Buoy 42 continues to maintain intensity around 40 knots. The Froude number is less than unity after 0600Z on January 26, therefore, a barrier jet could form at this time. The barrier jet can be shown existed during the entire time due to the fact the winds were in excess of 40 knots at Buoy 42 to 1800Z on January 26 by which time the winds continue to have wind gusts above 10 ms^{-1} (20 knots) but less than 15 ms^{-1} (29 knots) until 0000Z on January 27. The winds at Buoy 42 begin to show an increase again around 0700Z, on January 27, with the maximum increase happening around 0900Z with a wind speed gust of 22.4 ms^{-1} (43.4 knots). This increase in wind speed happened as the pressure field orientation rotated into more of an along-coast direction. Also at this time, the Froude number is low with values around 0.60 to 0.83 indicating a blocked flow response. The winds continued to be strong albeit not as strong as 22.4 ms^{-1} (43.4 knots) but in the range between 10-17 ms^{-1} in wind strength from the southeast until the shortwave trough passed through Buoy 42 at 0300Z on January 28, the time when the low pressure makes land fall in Northern California.

The observations at the Monterey Airport showcased some interesting uniqueness during this storm period. The winds at Monterey remained light and variable from the east through most of January 25. The winds

at Monterey were very low with the winds finally gusting to 21 knots at 2000Z on January 25. The Froude number from 1500Z through 2100Z on January 25 was greater than unity, which would allow down-mountain flow in the lee of the topography. Figure 21 shows the mesoscale pressure distribution at 1800Z on January 25 and indicates a strong cross-coast pressure gradient. High winds along the coast are supported by a geostrophic response to this pressure gradient. The mesoscale low-pressure trough over the Monterey Bay would support some down-gradient flow for unblocked conditions. This is consistent with an increase in southeast flow at the Monterey Airport at this time.

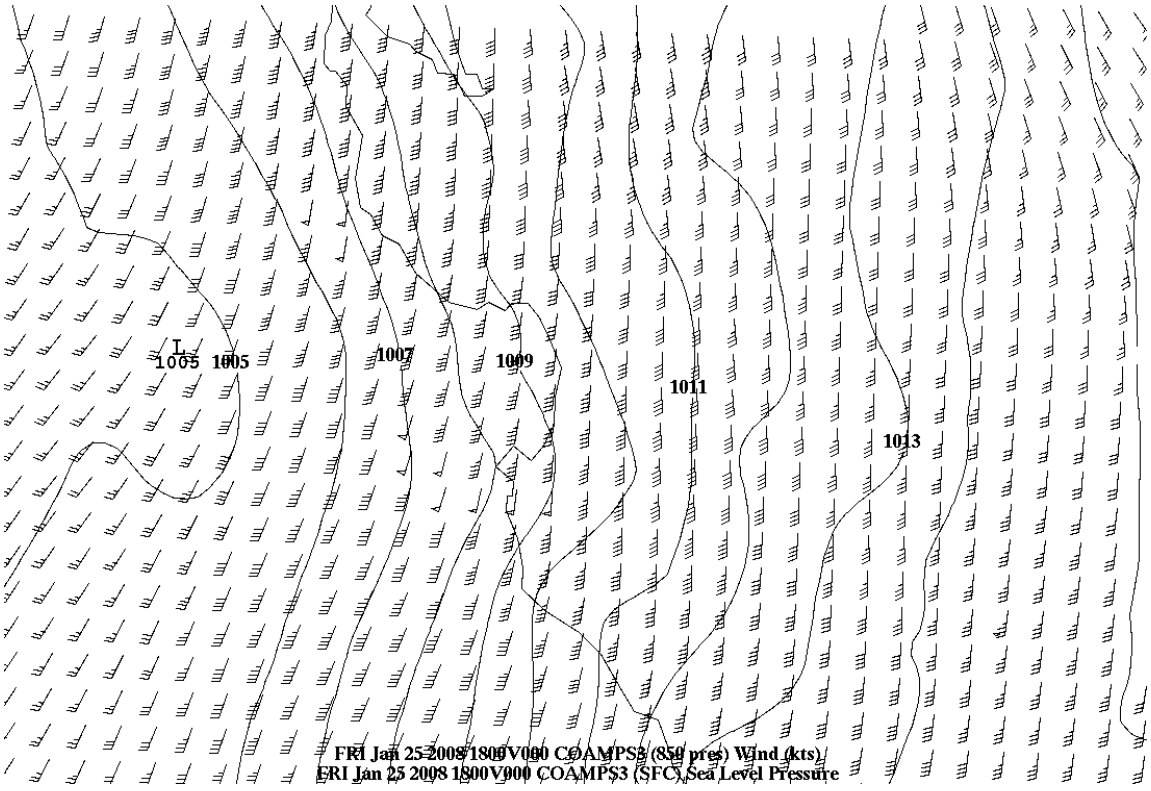

Figure 21. Winds at 850 hPa coming from a southerly direction with a mesoscale low center west of the Monterey Bay, helping the winds to have a slight easterly component at the surface.

The winds did not show another speed increase until 0700Z-0800Z on January 26 at the Monterey Airport. The winds did not blow strong at the

Monterey Airport due to the fact the Froude number at 0000Z on January 26 was less than unity. The Froude number was greater than unity starting at 0300Z but the winds did not pickup in intensity until the winds had hit their maximum of 50 knots from the south at 850 hPa around 0600Z-0700Z on January 26. The Froude number was greater than unity at 0300Z and 0600Z, respectively, which again supports an increase in down slope flow near the Monterey Airport with the weak pressure trough in the Monterey Bay region persisting during this time (Figure 22).

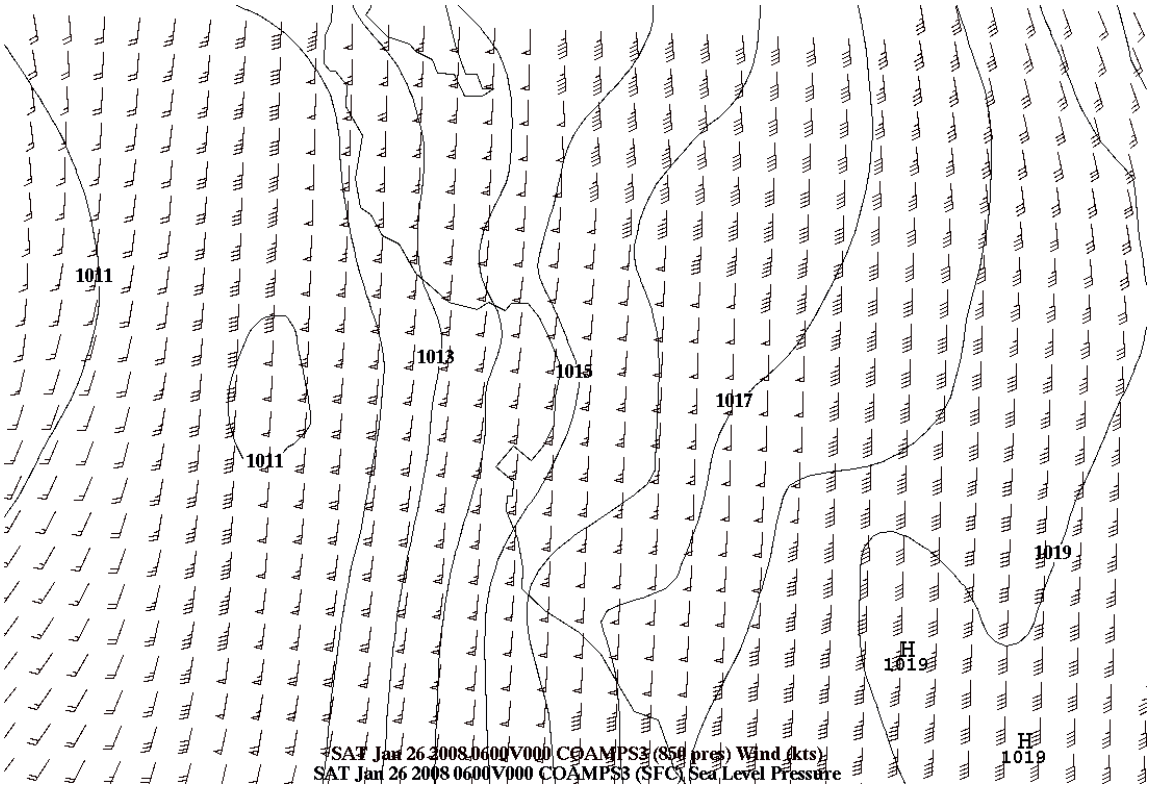

Figure 22. The wind--increasing over the Monterey Peninsula, at 850 hPa, to around 55 knots by 0600Z on January 26—which helped to trigger the southeasterly winds that occurred at the Monterey Airport at 0800Z, with wind gusts approaching 20 knots.

By 0900Z, the Froude number started a significant decrease to values, around 0.268, by 1200Z on January 26. At the same time the winds at the Monterey Airport, at 1200Z on January 26, had decreased to calm winds and

continued to be fairly calm for the rest of the day. By the end of January 26, the winds increased with wind gusts around 15-17 knots from an easterly direction. The winds at Buoy 42 at this same time had wind speed gusts that were greater than 40 knots until 1800Z on January 26 and were at least 30 knots in wind speed gust until 0000Z on January 27. With the decreasing Froude number through the first 12 hours coupled with the fact that the winds were also decreasing in strength aloft. Evidence suggests a barrier jet had been established along the Central California coastline, which allowed the winds to maintain intensity at Buoy 42.

The fact that the winds are adjusting to the SLP orientation on January 26 in an ageostrophic way, which allows the surface winds to come from an east by north-east fashion towards the lower pressure that is situated to the southwest of the Monterey Peninsula (Figure 23).

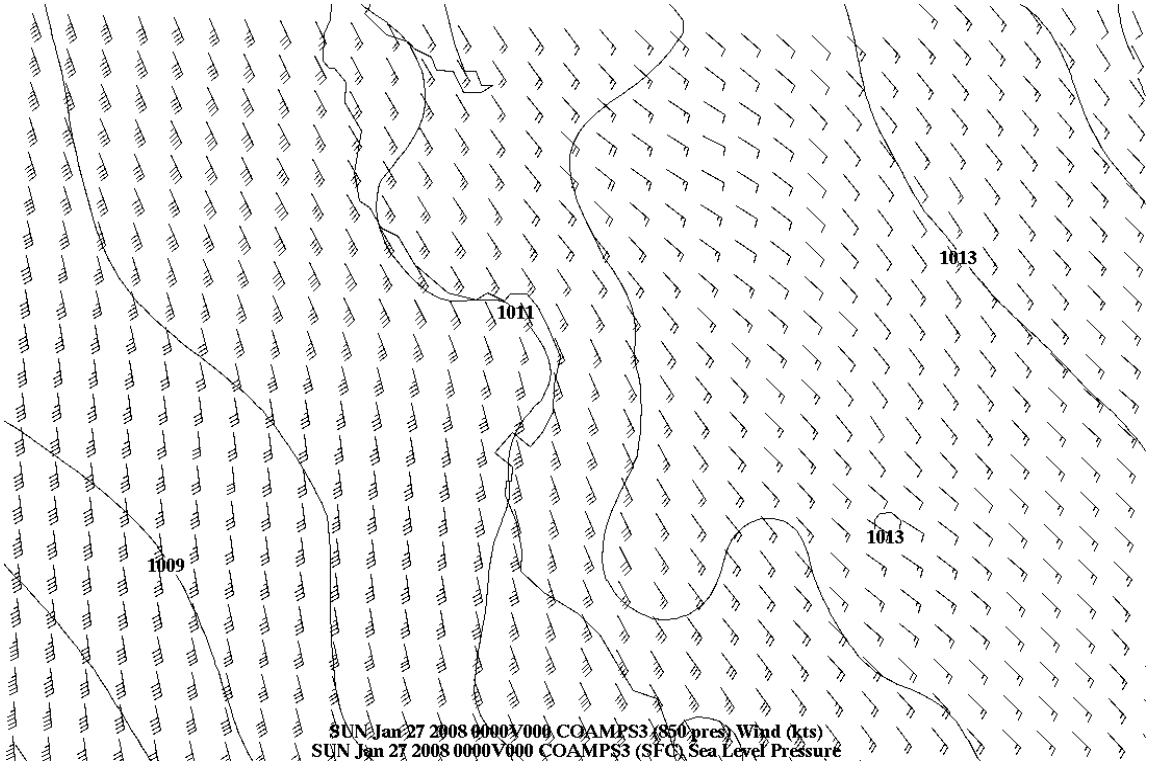

Figure 23. Winds at 850hPa from a southeast direction. Notice the alignment of the SLP contours with the coastline of California. The lowest pressure is to the southwest of the Monterey Peninsula.

The wind speeds, at the surface on January 27, began originally from an easterly direction but slowly turned and came from a southeast direction by 1000Z at the Monterey Airport. During this timeframe the Froude number increases to values around 0.68 (Figure 24).

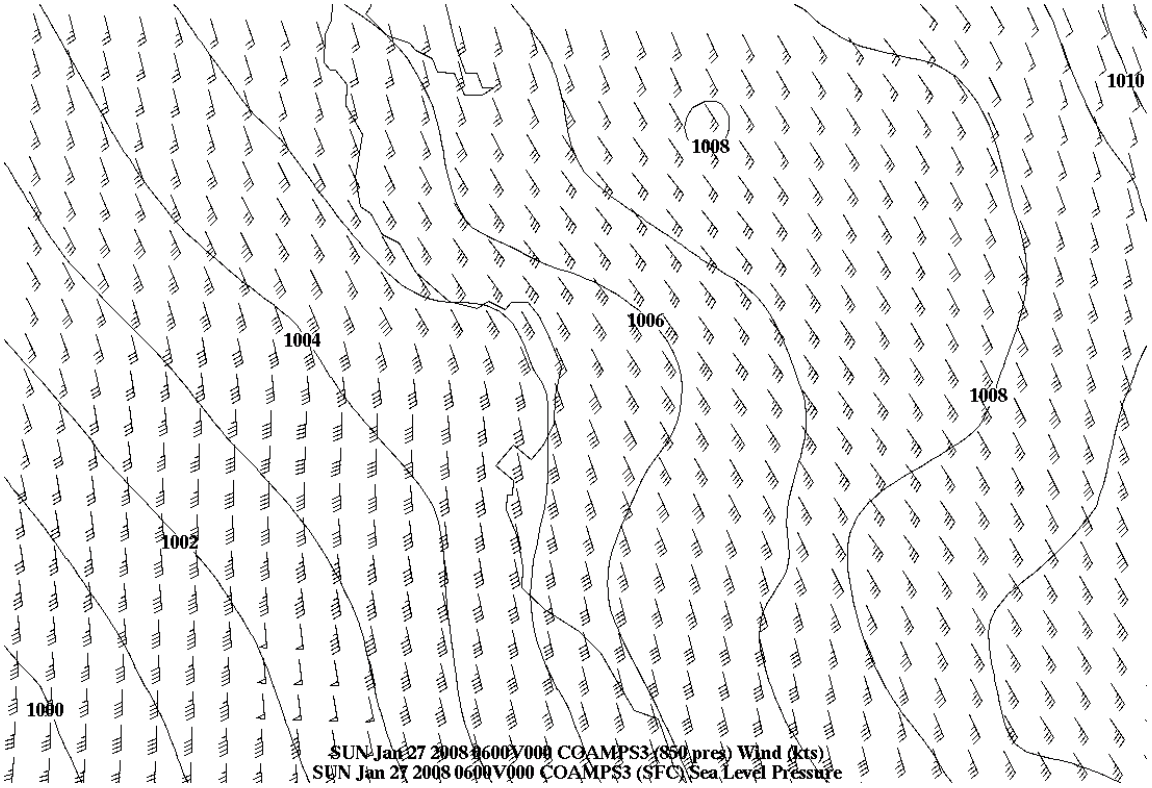

Figure 24. Winds at 850 hPa are from a southeast direction at 0600Z on January 27.

Winds between 1200Z and 1800Z on January 27 become weaker again with the Froude number still below unity even though the flow has a more favored onshore component of 200-230 degrees. The pressure gradient between the hours of 1200Z and 1800Z on January 27 show a south to north orientation. By 2100Z the flow is still blocked but the Froude number is now at 0.856. The winds at Buoy 42 are high from 0900Z through 1200Z on January 27 with wind speed gusts greater than 40 knots. At 1800Z the winds at Buoy 42 are around 30 knots in wind speed gust. By 0000Z on January 28 the Froude

number is 1.2 and the winds have started to blow from a south by southeasterly direction with the wind speed gust reading as high as 28 knots at the Monterey Airport. The 850hPa winds are now from a southwest direction. Even though the wind speeds are lower, the direction is from a more favorable onshore direction and that allows the winds to move over the northern sections of the Santa Lucia mountain range. This pressure pattern is similar to case 1 and produces a similar but weaker response. Winds continue to switch to the west and by 0530Z the low moves onshore and the pressure gradient relaxes (Figure 25).

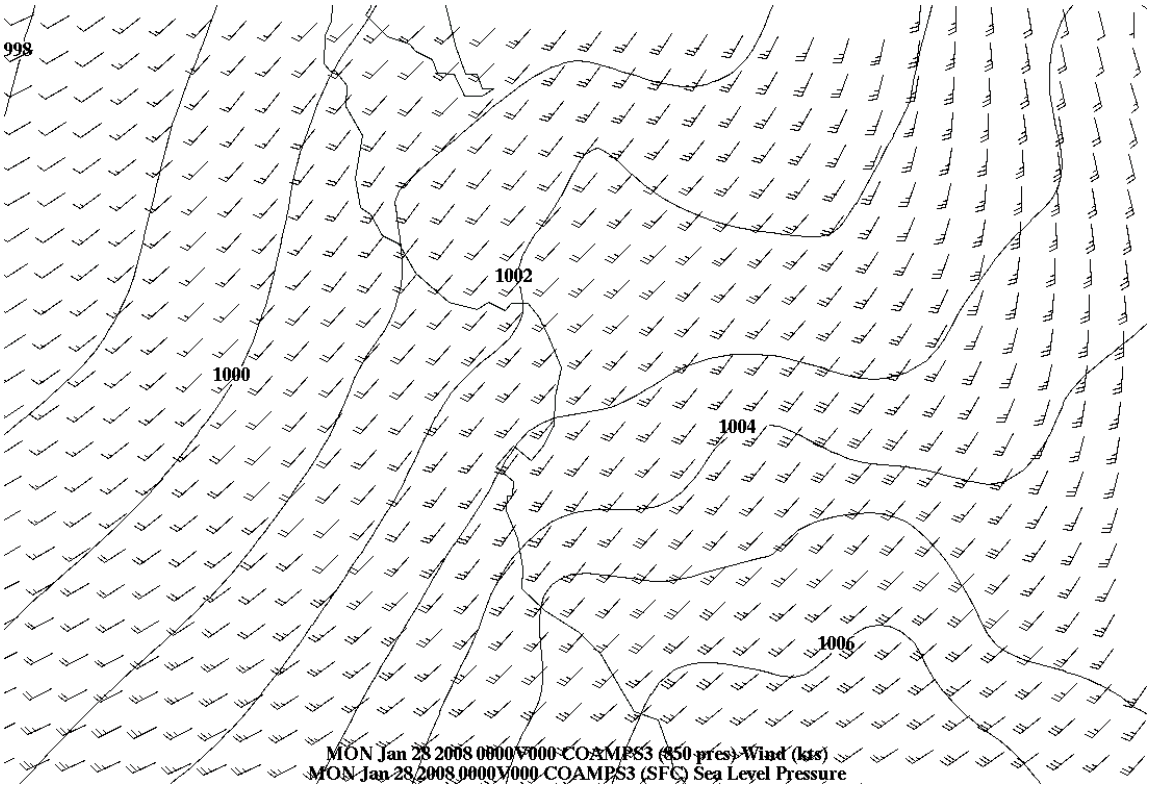

Figure 25. Winds at 850 hPa on January 28 at 0000Z have now switched direction and are coming from the southwest. The switch allows the winds to gain in strength at the Monterey Airport.

Winds at the Salinas Airport showed some of the same characteristics that the winds were displaying at Buoy 42. The winds started on the January 24 from the southeast with speeds slowly increasing through the day

and peaking at 28 knots at 1900Z on January 24. The winds early on January 25 were not very strong for the first 12 hours. The direction was from the southeast and the sustained wind speed was around 15 knots. After 1200Z the winds started to show a strong increase to a maximum of 39 knots in a wind gust at 1800Z. The wind gusts continue to be from the southeast and the speed of the wind gusts was around 30 knots until 1200Z on January 26. After 1200Z on January 26 the winds at Salinas are from the east-southeast with wind gust speeds up to 26 knots. The winds were not as strong late on January 26 and into January 27 because the 850hPa flow, in the Salinas valley at that time, was much weaker aloft than the flow was when the high winds arrived on January 25 and January 26. Another consideration is that the pressure field orientation had an orientation that had a more onshore component on January 27 which did not align well with the Salinas Valley and corresponded to weaker wind flow through the Salinas Valley.

3. Case 3 (February 23-25, 2008)

a. Introduction

Case 3 was another land falling frontal case that exhibited some similarity to case 1. The buoys showed a characteristic ageostrophic barrier jet along the Central California coastline, while the Monterey Airport only got high winds when the flow became unblocked. Salinas Airport exhibited a gap flow response with high winds occurring at similar times to the barrier jet that was located offshore.

b. Synoptic Overview

This weather event had a filling low that eventually made landfall around Cape Mendocino in Northern California. Some strong Southerly winds were associated with this weather feature as it approached the California coastline. The storm started out with an upper-level trough situated over the eastern Pacific Ocean, and with an upper-level ridge over the Eastern Sections of the inner-mountain west region of the United States. A shortwave ridge was

embedded in the upper-level trough that was just off the coast of the United States on February 23 at 0000Z. At the surface, a 990hPa low was to the west of the shortwave ridge. The low was due west of Los Angles by about 1160 Nautical Miles on February 23 at 0000Z. At 1200Z, on February 23, the low moved in a northeasterly fashion and was located 685 miles due west of Monterey. The pressure gradient had increased dramatically around the low because the low pressure had deepened to 971 hPa low. Much of the strong pressure gradient, at that time was still centered over the water region of the Eastern Pacific Ocean (Figure 26 and Figure 27) and winds were low over the Monterey Bay region.

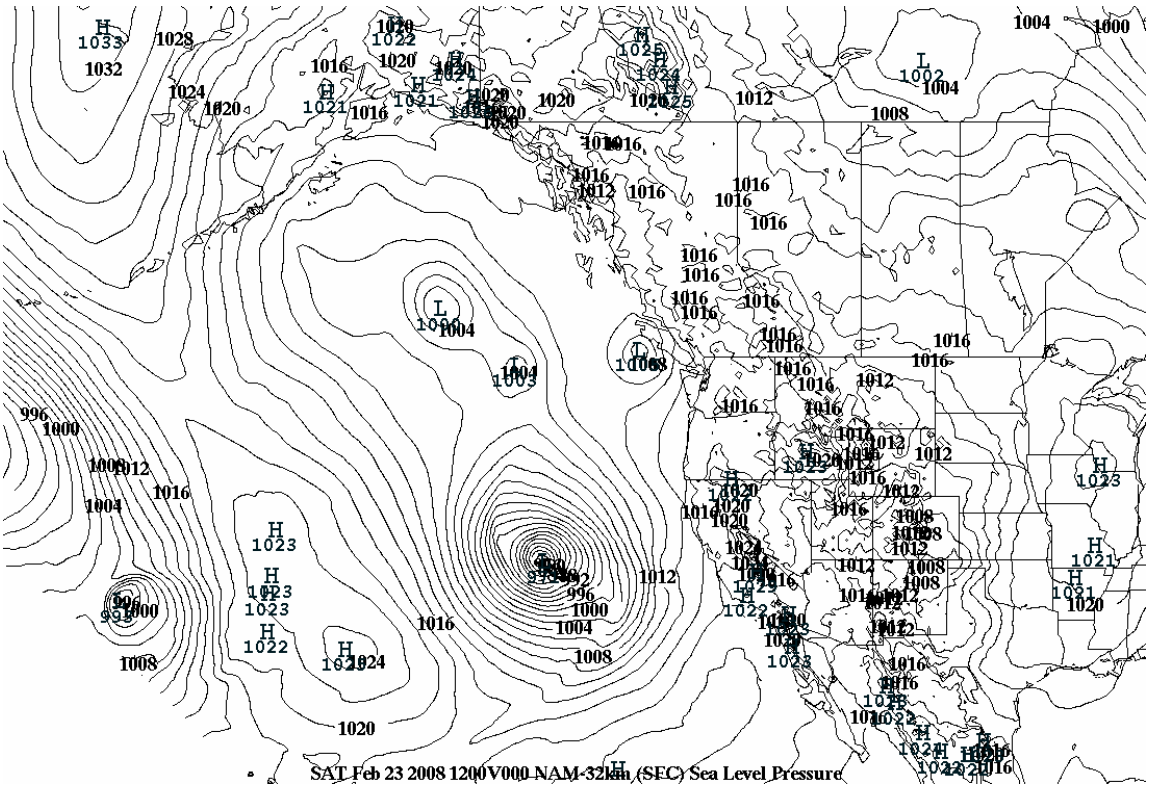

Figure 26. The deep low to the west of California in the Eastern Pacific Ocean at 1200Z on February 23.

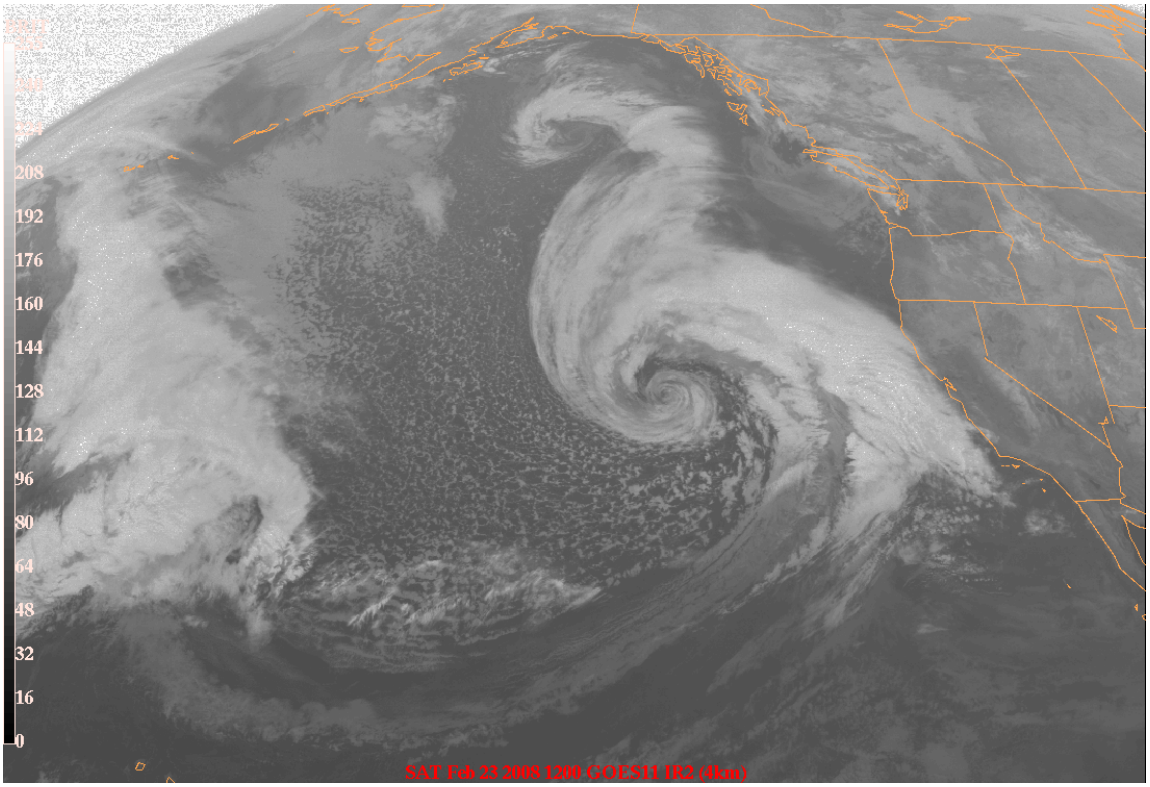

Figure 27. IR satellite image for 1200Z on February 23 which displays where the low-pressure center is located.

On February 24 at 0000Z, the low had started to fill as it was becoming barotropic. The low became vertically stacked and had a central pressure of 973hPa. The pressure gradient during this time frame became much tighter over the Central Coast of California (Figure 28 and Figure 29). The winds along the Central Coast of California started to increase especially at Buoy 42. The winds at 1200Z, on February 23, were from the southeast at 5 ms^{-1}, but by 1600Z, on February 23, the winds were still from the southeast with wind speed gusts approaching 15 ms^{-1} (29 knots). The pressure gradient continued to increase over the Central Coast of California with wind speed gusts reaching 21 ms^{-1} (41 knots) by 0000Z on February 24.

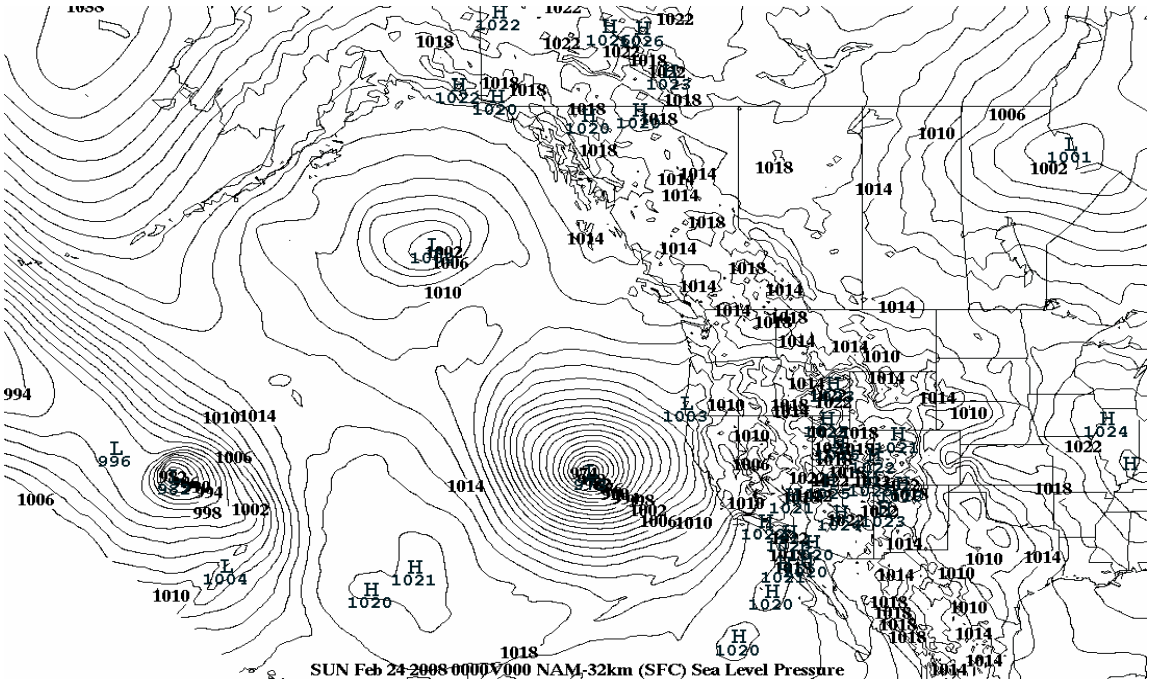

Figure 28. The low has moved northeastward over the last 12 hours helping to tighten the pressure gradient over the Central California coastline. The chart is valid at 0000Z on January 24.

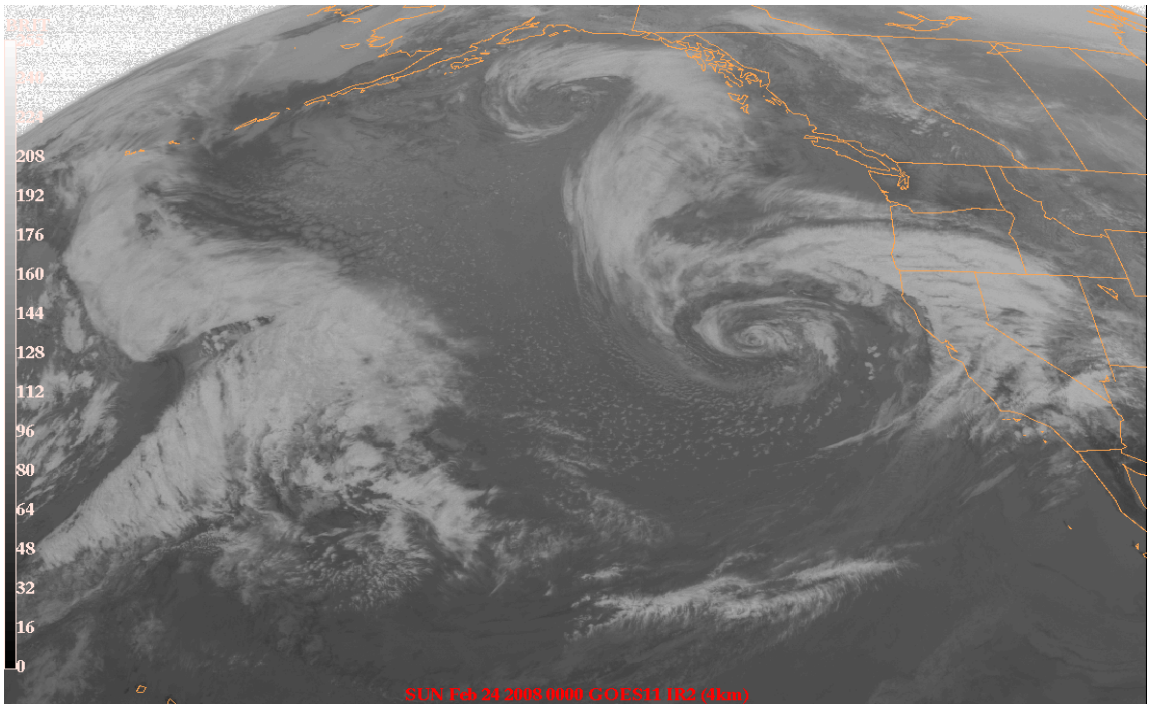

Figure 29. IR satellite imagery shows the front moving through the Monterey Bay region of California at 0000Z on February 24, when the strongest winds occurred at the Monterey Airport.

At 1200Z on February 24, a shortwave trough had developed over water and it was very close to the low-pressure center. This shortwave trough helped to produce strong winds again from a southerly direction, around the Monterey Peninsula. The winds increased when the shortwave trough approached the Monterey Bay region (Figure 30 and Figure 31). The orientation of the pressure field produced a flow that has a more onshore component versus having a component that is more coast parallel.

Figure 30. SLP field at 1200Z that shows the low continuing to fill and the SLP field maintain its strength over the Monterey Peninsula.

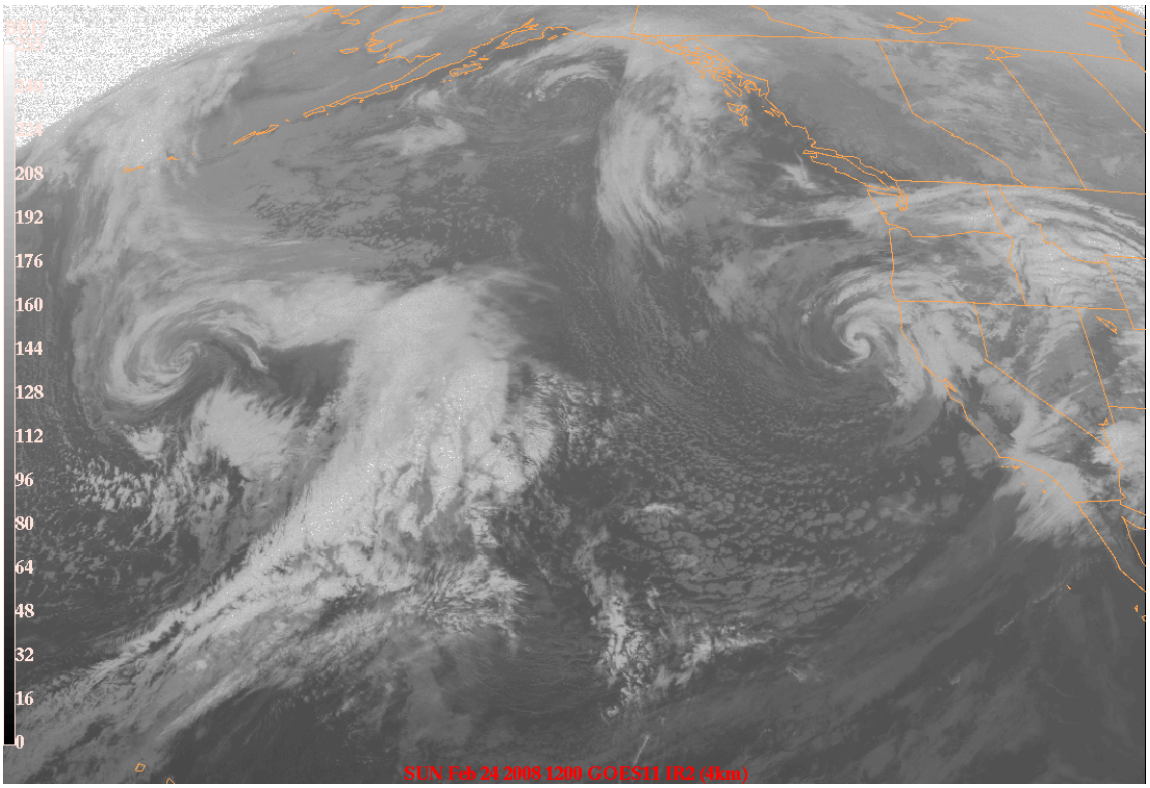

Figure 31. The low pressure center on the IR satellite image at 1200Z on February 24 shows how the low is filling as it continues to the northeast.

The low-pressure center kept moving on a northeasterly track on a collision course with the California-Oregon border at 0000Z on February 25. The low continued to weaken and fill as it moved over land in a Northeasterly fashion.

It attained a 1002hPa pressure low along the western sections of the California-Oregon border. The winds finally dropped in strength at 0000Z on February 25 when the low made landfall along the Oregon-California border with wind speeds around 10 knots in strength (Figure 32).

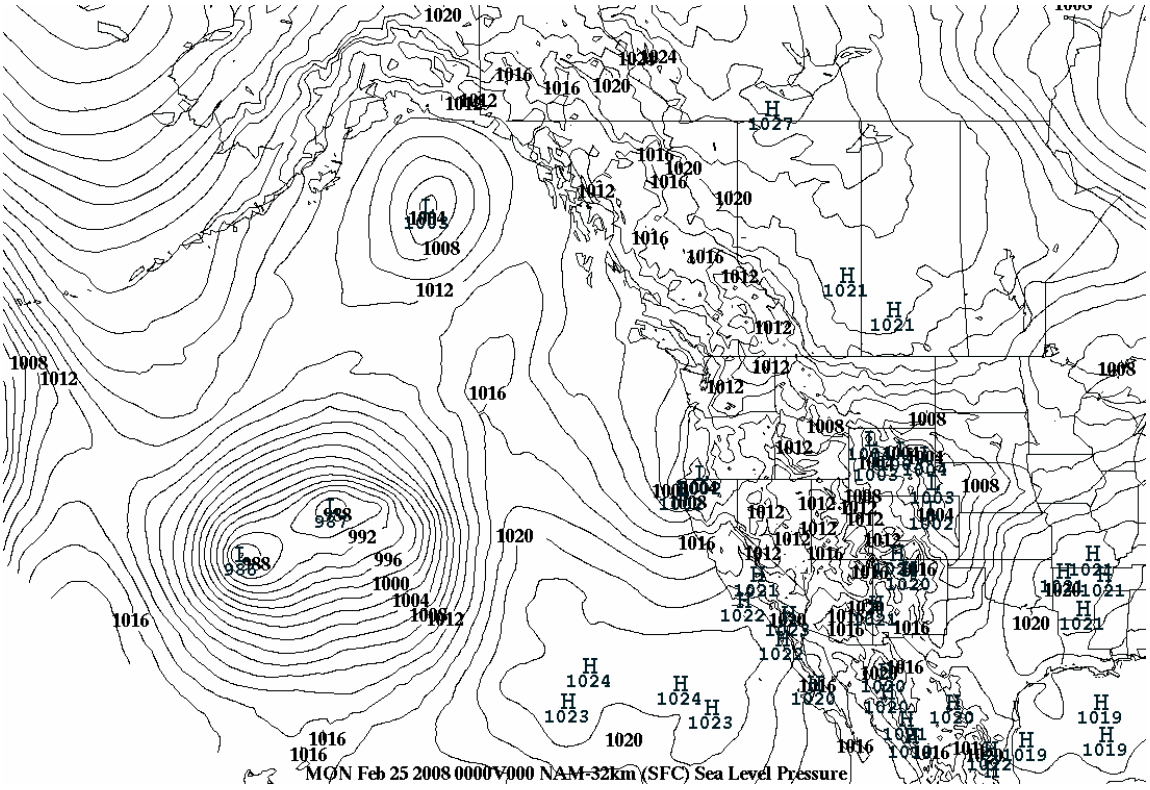

Figure 32. SLP field at 0000Z on February 25 that shows the low making landfall along the Oregon-California border.

c. Mesoscale Effects Around the Monterey Peninsula Region

Wind speeds, for case 3, had some of the same characteristics that were present in case 1. The winds, at Buoy 42 on February 23 at 1300Z, are from the south but only at 3 ms^{-1}. Over the next 5 hours, until 1800Z on February 23, the winds increase and rise to about 11 ms^{-1} (21 knots) from the southeast as the deep low well offshore moved closer to the coast. Over the next 6 hours until 0000Z on February 24, the winds peak at 21.5 ms^{-1} (42 knots).

This time frame correlates with the cold front passing through the region as depicted on the satellite imagery. From 0000Z to 1800Z on February 24, the winds continue to blow from the south with wind gusts in the vicinity of 15 ms^{-1} (29 knots) +/- 2 ms^{-1} (3.9 knots). The south winds occurred even though it was post-frontal because the pressure gradient remained in the same along coast orientation. By 1800Z, the wind starts to switch direction and blow from the southwest as the shortwave trough has moved through the region.

Monterey Airport had some differences compared to when the wind blew at Buoy 42 on February 23 through February 24. The winds at the Monterey Airport were light and variable until late in the day on February 23 when the 850hPa winds increased and the cross-coast pressure field gradient increased (Figure 33).

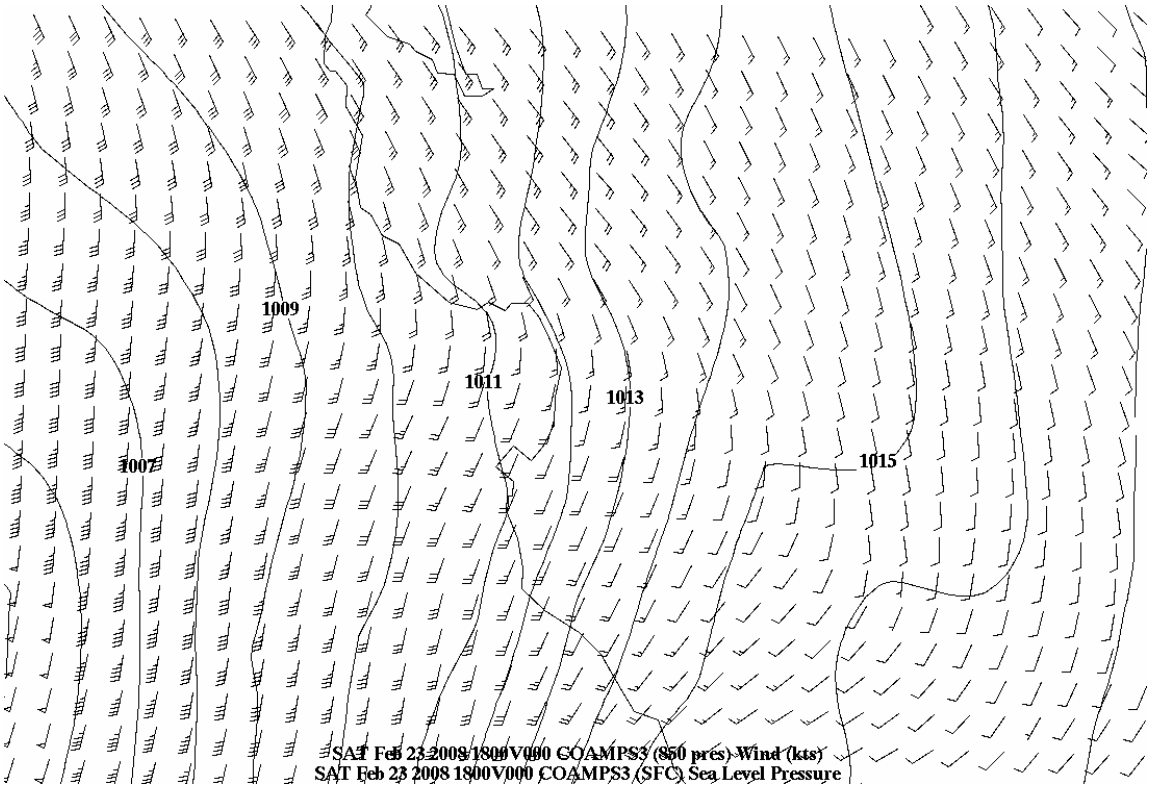

Figure 33. The 850 hPa winds over the Monterey Peninsula (shown with the SLP contours at 1800Z on February 23) have a Froude number less than unity.

The winds finally start to show some strength, in the form of gusts greater than 20 knots from the southeast, starting around 2100Z on February 23. This time corresponds with the time when the Froude number becomes greater than unity at 2100Z on February 23, which supports a down-gradient down slope flow in the lee of the mountains south of the Monterey Airport. The strongest of these winds occurred around 2330Z on February 23 with a wind speed gust of 39 knots. The 39 knots relates to the time of cold front passage that took place, with this weather system at the Monterey Airport around 0000Z on February 24 (Figure 34) and the winds at 850 hPa reached their maximum. As seen in Figure 35, a mesoscale low-pressure region occurs in the Monterey Bay to help produce a north-south pressure gradient that supports ageostrophic down-gradient southeasterly flow near the Monterey Airport.

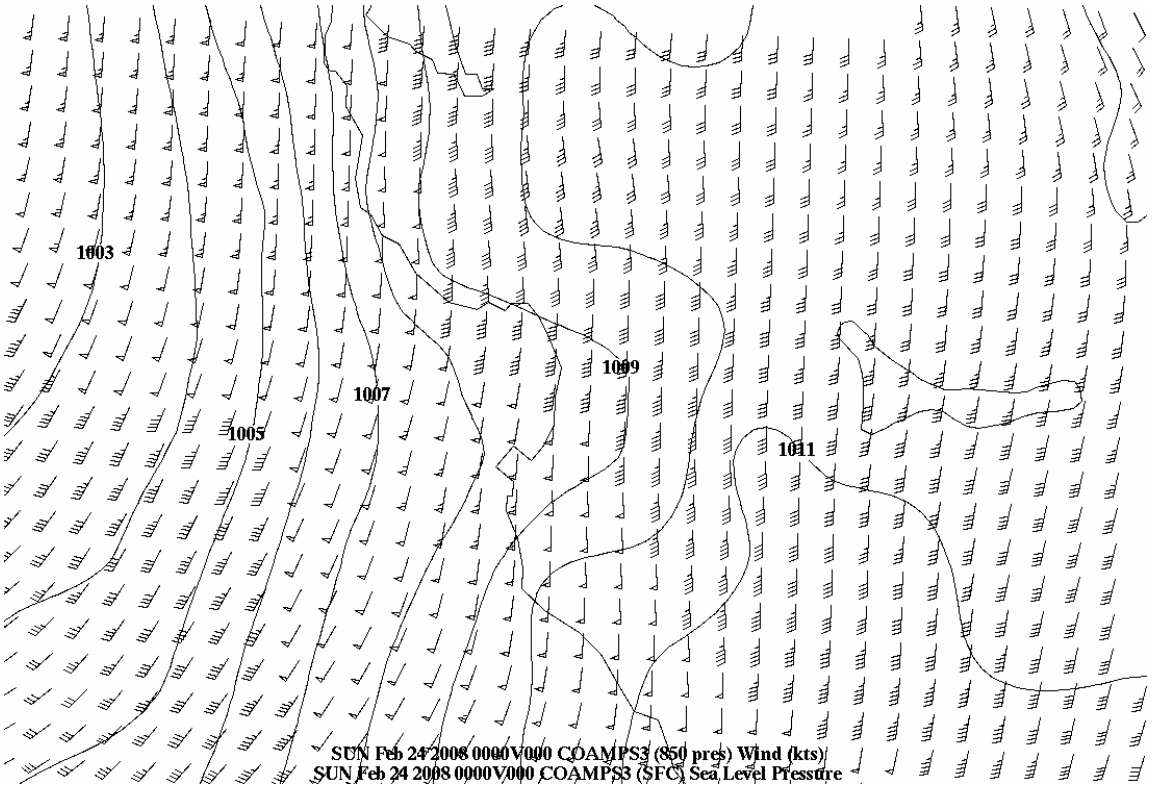

Figure 34. Winds speeding up over the Monterey Peninsula at 850 hPa on February 24 at 0000Z to 50 knots. Also the low level jet of 50 knots signifies the placement of the frontal boundary at 0000Z on February 24 over the Monterey Peninsula.

The winds then die down from 0300Z to 0600Z to the single digits but continue to be from the southeast at the Monterey Airport. Then the winds begin to ramp up to around 15 knots sustained wind speed, with wind speed gusts up to 33 knots, as the shortwave trough approaches and then passes thru the Monterey Airport (Figure 33 and Figure 34). The orientation of the pressure field allowed for the winds to remain strong after the front moved through the region at 0000Z on February 24. The winds at the Monterey Airport finally calm back down to around 10 knots starting around 0000Z on February 25.

The airport at Salinas had wind speeds that were even stronger than the winds at the Monterey Airport. The interesting feature, regarding the winds at Salinas and Monterey, was that the arrival time, of peak winds at the Salinas Airport, was earlier than the arrival time of peak winds peaked at the Monterey Airport. At 1200Z, on February 23, the winds were from the southeast at around 10 knots at the Salinas Airport. Over the next 7 hours the winds ramped up to have sustained wind speeds above 30 knots, with wind gusts over 40 knots on February 23. The winds continued to be strong at the Salinas Airport, until 0600Z, on February 24, where the direction is from the southeast with wind gusts reaching 25 knots. After this time, the winds continue to be blustery but only at wind speeds less than 25 knots with a direction from the southeast. The wind direction begins to turn to the southwest by 2100Z on February 24 with the wind gusts around 20-23 knots. The wind speed gust strength correlates very well to the timing that happened with the winds that occurred at Buoy 42 (Figure 35).

Both locations (Salinas Airport and Buoy 42) had winds that began to intensify between the hours of 1500Z and 1800Z on February 23. Both locations also had their respective maximum wind gusts around 2100Z while the maximum winds at the Monterey Airport occurred at 2330Z. Another key fact to the strong winds had to deal with the orientation of the pressure field in the Salinas valley. The peak winds hit with the pressure field having the largest

along valley gradient between the hours of 1800Z on February 23 through 0200Z on February 24 (Figure 37). The alignment allowed for higher wind speeds to occur at the Salinas Airport during this time.

The winds along the Big Sur coastline, at the beginning of the storm, were blocked, as indicated by the Froude number (0.6351) for flow coming into the area at 1800Z on February 23. The winds at Buoy 42 show a slight increase with a gust of 14.4 ms^{-1} (28 knots) at 1700Z on February 23. The winds at that time at the Monterey Airport were only at 5 knots with a compass heading of 080 degrees. The response at the buoy showed a barrier jet starting to establish itself along the coastline ahead of the approaching front. The barrier jet was short-lived because the flow turned to have a slightly more onshore component and the flow then became "unblocked" at 2100Z on February 23 as the front gets closer and the flow direction changes to a more onshore flow. The flow remains "unblocked" after the front goes through and stability decreases, which continues until 2100Z on February 24 when the winds start to have wind speeds less than 10 knots.

D. SUMMARY OF RESULTS FOR THE THREE CASES

The three weather cases that produced strong winds around and on the Monterey Peninsula had some similar characteristics as well as some dissimilar characteristics. The two frontal cases (case 1 and case 3) displayed the same tendencies of the strong winds in all three locations analyzed to produce strong winds along the Big Sur Coastline, the Monterey Airport, and the Salinas Airport. Case 1 displayed results that followed this pattern. The winds, when blocked, had higher velocities over the coastal waters than observed at the Monterey Airport, which could be seen by the Buoy 42 wind observations. Once the flow became "unblocked" (when the Froude number became greater than unity), the flow has the same strength at Buoy 42 as it has at the Monterey Airport. Case 3 also had some of the same tendencies, i.e., before frontal passage, the winds were not strong from a southerly direction at the Monterey Airport until the flow

became “unblocked.” Case 2 did show a tendency towards the same patterns as cases 1 and 3, but the wind flow observed at the Monterey Airport, was primarily an easterly flow, not a southerly flow. The reason the Froude number technique did not work as smoothly as in the other cases was twofold. The direction of the surface pressure gradient was almost in perfect alignment with the coastal topography. So there was no real windward ridging or a lee trough being produced in the atmosphere along the Santa Lucia mountain range that would influence the winds at the Monterey Airport. Also the alignment was such that the high pressure was further to the east than to the south and the wind flow was directed towards a westerly direction versus a northerly direction. Case 2 did provide some insight into the application of a Froude number analysis. When the Froude number was greater than unity, the wind blew from a southerly direction at the Monterey Airport. The Froude number is a good indication of when to expect strong winds at the Monterey Airport when a reasonably strong north-south pressure gradient occurs over the south part of Monterey Bay.

The other goal of this study was to see how the topography influenced the winds in the Salinas Valley. The winds that took place at the Salinas Airport for the three cases had some interesting properties. Case 1 had winds that were strongest at 1200Z with a peak wind gust of 39 knots compared with a wind gust of 49 knots at Monterey that occurred at 2200Z on January 4. Case 2 had wind speeds around 40 knots but the winds did not “peak” at Monterey until two hours later, with a reduced wind speed near of 21 knots. Case 3 had the same tendency in that the winds at the Salinas Airport “peaked,” at 44 knots, two to three hours earlier than the winds at the Monterey Airport. For the wind to be able to pick-up in wind speed the Froude number needs to be greater than unity at the Monterey Airport, but for the wind speeds to pick-up at the Salinas Airport the Froude Number was not indicative of the forcing. More important at the Salinas Airport is with the northwest-southeast pressure field alignment that would drive a gap flow response in the Salinas Valley. The Salinas Airport winds

were caused by a gap flow response versus a Froude number response that was present in the winds that blew at Buoy 42 and at the Monterey Airport.

The winds at Salinas did correspond with the simplistic regression equation, but the spread in the strength of these winds was a quite large with an 18-knot range for a 95% confidence interval. All three cases followed the trend of having strong winds at the Salinas Airport before the winds actually blew with strength at the Monterey Airport, every time. Looking at all 16 wind events, Salinas had strong wind speed periods that happened there sooner than similar events happened at the Monterey Airport. This observation is for all weather systems that were approaching from the west that were in the scope of this research. The Santa Lucia mountain range acted as a blocking mechanism for the Monterey Airport.

V. CONCLUSIONS AND RECOMMENDATIONS

A. CONCLUSIONS

This thesis project examined the Central California Coastal Jet in land falling storms, and its interactions with topography. Possible cases for Central California Coastal Jet for the years of 2005 to 2008 were identified based on a simple wind speed criteria. Eighteen events were found to meet the criteria for case studies, which were then whittled down to three cases that were studied exclusively to characterize the topographic forcing. The 18 storms with coastal jet events could be classified into two groups: cut off low and land falling fronts. The land falling fronts group was then subdivided into two categories: (1) fast moving fronts and (2) stalling fronts or extended gradients. All three cases chosen for detailed analysis happened during the year of 2008 in the months of January and February.

The first case took place during the January 3 through January 5 time interval. This case was identified as a land falling frontal case with a sub category reading of an extended gradient. Also, this case included the most extreme wind gust reported at the Monterey Airport with a wind gust of 49 knots. The first case highlighted the possibility that a mesolow that the storm produced in the Monterey Bay might have helped to produce stronger than normal winds on the Monterey peninsula. In addition, the Froude number technique worked extremely well in this case and helped to identify when winds would begin to intensify at the Monterey Airport.

The second case happened during the January 25 through January 28, and it was classified as a cut off low case. Also the second case had the longest storm duration found in the three cases chosen for detailed study in this thesis. This case highlighted that the direction of flow is very important for predicting if and when high winds might occur along the Monterey Peninsula. Coast parallel geostrophic flow as observed in this case produced very little high wind response

at the Monterey Airport. This case also showed that the Froude Number technique is not a foolproof forecast technique that will work without fail.

The third case highlighted another frontal case that moved through the region on February 23 through February 25. This case had a very fast moving frontal feature that accompanied it while the first case had a slower moving frontal feature so this case was in the fast moving front group. Also, this case highlighted that the winds in the Salinas Valley (especially at the Salinas Airport) will show an increase in wind speed sooner than the winds at the Monterey Airport. In addition, the winds at the Salinas Airport will increase in strength around the same basic time the winds begin to pickup in speed at Buoy 42.

The thesis found some very good correlations between the measured and calculated wind speeds around the Monterey peninsula. First, winds at the Monterey Airport, which blow over 25 knots from a southerly direction and are in the land falling fronts group, occur only when the Froude number is greater than unity. Second, the wind speed gust can be predicted with some accuracy by using a now-casting technique that uses pressure measurement, at the Monterey Airport and at the Salinas Airport, in a linear relationship between pressure gradient and wind speed. Third, the Central California Coastal Barrier Jet can exist under conditions that do not include a frontal feature as which existed in case two. Fourth, with land falling frontal features, the wind direction of the 850 hPa flow is very important to the determination of whether specified winds have the potential to be strong at the Monterey Airport.

B. RECOMMENDATIONS

To identify specific weather conditions, which produce strong winds along the Central California Coastal region, a larger historical study of weather systems that have hit this coastal region needs to be completed. The scope of this study only covered the years from 2005 thru 2008. A more robust study is necessary to see generalized weather patterns that may emerge over the Central California Coastal region. Also more case studies need to be done on cut-off lows as well

as land falling frontal features that hit the Central California Coastal region. The time period, for data acquisition, should be extended to include data for at least the last 10 (if not the last 30) years for a more complete look at wind events that happened along the Central California Coastal region.

Another area for improvement is development of an automated Froude number calculation, using model output, to better aid weather forecasters when they need to predict whether wind will flow over topography and into the city of Monterey. With an automated program, the weather forecaster could make earlier forecasts of wind speed and direction at the Monterey Airport.

The Froude number technique that was used in this thesis could be applied to other regions of the world for better predictions of when winds hit on the lee side of mountain slopes. A good candidate would be the city of Anchorage, Alaska, where the mountain range to the south of the city “blocks” the flow over topography. A study could be done to see whether a Froude number larger than unity correlates with high winds in the city of Anchorage.

THIS PAGE INTENTIONALLY LEFT BLANK

LIST OF REFERENCES

Bond, N. A., B. F. Smull, M. T. Stoelinga, C. P. Woods, and A. Haase, 2001: *Evolution of a cold front encountering steep quasi-2D terrain: Coordinated aircraft observations on 8–9 December 2001 during IMPROVE-2.*

Blier, W. 1996: A numerical modeling investigation of a case of polar airstream cyclogenesis over the Gulf of Alaska. *Monthly Weather Review, 124*(12), 2703-2725.

Colle, B. A., K. A. Loescher, G. S. Young, and N. S. Winstead, 2006: Climatology of barrier jets along the Alaskan coast. part II: Large-scale and sounding composites. *Monthly Weather Review, 134*(2), 454-477.

————, and C. F. Mass, 1998: Windstorms along the western side of the Washington cascade mountains. part I: A high-resolution observational and modeling study of the 12 February 1995 event. *Monthly Weather Review, 126*(1), 28-52.

————, and ————, 1998: Windstorms along the western side of the Washington cascade mountains. part II: Characteristics of past events and three-dimensional idealized simulations. *Monthly Weather Review, 126*(1), 53-71.

————, and ————, 2000: High-resolution observations and numerical simulations of easterly gap flow through the Strait of Juan de Fuca on 9–10 December 1995*. *Monthly Weather Review, 128*(7), 2398-2422.

————, B. F. Smull, and M. Yang, 2002: Numerical simulations of a land-falling cold front observed during COAST: Rapid evolution and responsible mechanisms. *Monthly Weather Review, 130*(8), 1945-1966.

Doyle, J. D. 1997: The influence of mesoscale orography on a coastal jet and rainband. *Monthly Weather Review, 125*(7), 1465-1488.

————, and N. A. Bond, 2001: Research aircraft observations and numerical simulations of a warm front approaching Vancouver Island. *Monthly Weather Review, 129*(5), 978-998.

Ferber, G. K., and C. F. Mass, 1990: Surface pressure perturbations produced by an isolated mesoscale topographic barrier. part II: Influence on regional circulations. *Monthly Weather Review, 118*(12), 2597-2606.

Galewsky, J., and A. Sobel, 2005: Moist dynamics and orographic precipitation in northern and central California during the New Year's flood of 1997. *Monthly Weather Review, 133*(6), 1594-1612.

January 2008 Western North American Super Storm, 2009: Retrieved March/12, 2009, from http://en.wikipedia.org/wiki/January_2008_Western_North_American_super_storm

Junker, N. W., R. H. Grumm, R. Hart, L. F. Bosart, K. M. Bell, and F. J. Pereira, 2008: Use of normalized anomaly fields to anticipate extreme rainfall in the mountains of northern California. *Weather and Forecasting, 23*(3), 336-356.

Kim, J., and H. Kang, 2007: The impact of the Sierra Nevada on low-level winds and water vapor transport. *Journal of Hydrometeorology, 8*(4), 790-804.

Kingsmill, D. E., P. J.Neiman, F. M. Ralph, and A. B. White, 2006: Synoptic and topographic variability of northern California precipitation characteristics in landfalling winter storms observed during CALJET. *Monthly Weather Review, 134*(8), 2072-2094.

Lewitsky, J., A. Moses, and R. Ruehl, 2008. *January 3-6, 2008 Storm Summary/Case Study.* Unpublished manuscript.

Loescher, K. A., G. S. Young, B. A. Colle, and N. Winstead, 2006: Climatology of barrier jets along the Alaskan coast. part I: Spatial and temporal distributions. *Monthly Weather Review, 134*(2), 437-453.

Ludwig, F. L., D. K. Miller, and S. G. Gallaher, 2006: Evaluating a hybrid Prognostic–Diagnostic model that improves wind forecast resolution in complex coastal topography. *Journal of Applied Meteorology and Climatology, 45*(1), 155-177.

Lynott, R. E., and P. O. Cramer, 1966: Detailed analysis of the 1962 Columbus Day windstorm in Oregon and Washington. *Monthly Weather Review, 94*(2), 105-117.

Macklin, S. A., N. A. Bond, and J. P. Walker, 1990. Structure of a low-level jet over lower cook inlet, alaska. *Monthly Weather Review, 118*(12), 2568-2578.

————, Lackmann, G. M., and J. Gray, 1988. Offshore-directed winds in the vicinity of Prince William Sound, Alaska. *Monthly Weather Review, 116*(6), 1289-1301.

Mass, C. F., & M.D. Albright, 1985. A severe windstorm in the lee of the cascade mountains of Washington state. *Monthly Weather Review, 113*(8), 1261-1281.

————, S. Businger, M.D. Albright, and Z.A. Tucker, 1995. A windstorm in the lee of a gap in a coastal mountain barrier. *Monthly Weather Review, 123*(2), 315-331.

————, & Ferber, G. K. 1990. Surface pressure perturbations produced by an isolated mesoscale topographic barrier. part I: General characteristics and dynamics. *Monthly Weather Review, 118*(12), 2579-2596.

Mitchell, T. P., & W. Blier, 1997. The variability of wintertime precipitation in the region of California. *Journal of Climate, 10*(9), 2261-2276.

Neiman, P. J., P. O. G. Persson, F. Martin Ralph, D.P. Jorgensen, A. B. White, and D.E. Kingsmill, 2004. Modification of fronts and precipitation by coastal blocking during an intense landfalling winter storm in southern California: Observations during CALJET. *Monthly Weather Review, 132*(1), 242-273.

————, Ralph, F. M., White, A. B., Parrish, D. D., Holloway, J. S., & Bartels, D. L. 2006. A multiwinter analysis of channeled flow through a prominent gap along the northern California coast during CALJET and PACJET. *Monthly Weather Review, 134*(7), 1815-1841.

————, Wick, G. A., Ralph, F. M., Martner, B. E., White, A. B., & Kingsmill, D. E. 2005. Wintertime nonbrightband rain in California and Oregon during CALJET and PACJET: Geographic, interannual, and synoptic variability. *Monthly Weather Review, 133*(5), 1199-1223.

Nuss, W. A., & D.W. Titley, D. W. 1994. Use of multiquadric interpolation for meteorological objective analysis. *Monthly Weather Review, 122*(7), 1611-1631.

Olson, J. B., Colle, B. A., Bond, N. A., & Winstead, N. 2007. A comparison of two coastal barrier jet events along the southeast Alaskan coast during the SARJET field experiment. *Monthly Weather Review, 135*(8), 2973-2994.

Overland, J. E. 1984. Scale analysis of marine winds in straits and along mountainous coasts. *Monthly Weather Review, 112*(12), 2530-2534.

————, and N. A. Bond, 1995. Observations and scale analysis of coastal wind jets. *Monthly Weather Review, 123*(10), 2934-2941.

————, and B. A. Walter, 1981. Gap winds in the Strait of Juan de Fuca. *Monthly Weather Review, 109*(10), 2221-2233.

Parish, T. R. 1982. Barrier winds along the Sierra Nevada Mountains. *Journal of Applied Meteorology, 21*(7), 925-930.

Pierrehumbert, R. T., & B. Wyman, 1985. Upstream effects of mesoscale mountains. *Journal of the Atmospheric Sciences, 42*(10), 977-1003.

Ralph, F. M., P.J. Neiman, and R. Rotunno, 2005. Dropsonde observations in low-level jets over the northeastern pacific ocean from CALJET-1998 and PACJET-2001: Mean vertical-profile and atmospheric-river characteristics. *Monthly Weather Review, 133*(4), 889-910.

Reed, R. J. 1980. Destructive winds caused by an orographically induced mesoscale cyclone. *Bulletin of the American Meteorological Society, 61*(11), 1346-1355.

Smith, R., B. 1979. The influence of mountains on the atmosphere. *Advances in Geophysics, 21*, 87-230.

Steenburgh, W. J., & C. F. Mass, 1996. Interaction of an intense extratropical cyclone with coastal orography. *Monthly Weather Review, 124*(7), 1329-1352.

Winstead, N. S., B. Colle, N. A. Bond, G. Young, J. Olson, K. Loescher, et al. 2006. Using SAR remote sensing, field observations, and models to better understand coastal flows in the Gulf of Alaska. *Bulletin of the American Meteorological Society, 87*(6), 787-800.

Yu, C., and N. A. Bond, 2002. Airborne doppler observations of a cold front in the vicinity of Vancouver Island. *Monthly Weather Review, 130*(11), 2692-2708.

INITIAL DISTRIBUTION LIST

1. Defense Technical Information Center
   Ft. Belvoir, Virginia

2. Dudley Knox Library
   Naval Postgraduate School
   Monterey, California

3. Dr. Wendell Nuss
   Department of Meteorology
   Naval Postgraduate School
   Monterey, California

4. Dr. Qing Wang
   Department of Meteorology
   Naval Postgraduate School
   Monterey, California

5. Dr. Philip Durkee
   Department of Meteorology
   Naval Postgraduate School
   Monterey, California

6. Air Force Weather Technical Library
   14 WS/WXCP
   Asheville, North Carolina

7. Liam Lynam
   Santa Fe, New Mexico